

Final Technical Report

Novel strategies for ultrahigh specific activity targeted nanoparticles

DEFG0208ER64671

09/15/08 to 09/14/12

Principal investigator

Dr. Michael J. Welch

Recipient organization

Washington University School of Medicine

510 S. Kingshighway Blvd.

St. Louis, MO 63110

Consortium/teaming members

Dr. Karen L. Wooley (Co-PI) Texas A&M University. College Station, TX

Dr. John A. Katzenellenbogen (Co-PI) University of Illinois at Urbana-Champaign, Urbana, IL

Washing University

Dr. Dong Zhou; Dr. Dexing Zeng; Ms. Carmen S. Dence; Dr. Yongjian Liu

Texas A&M University

Dr. Nam S. Lee; Sandani Samarajeewa

University of Illinois at Urbana-Champaign

Dr. Vincent Carroll; Ms. Marketa Lebl-Rinnova

Acknowledgments

This work is supported by the U.S. Department of Energy under Award No. DEFG0208ER64671

Note: any opinions, findings, and conclusions or recommendations expressed in this material are those of the authors and do not necessarily reflect the views of the Department of Energy (DOE)

1. Executive Summary

Nano-particles provide a unique and powerful platform for medicinal application. This project has looked into a novel and efficient way to label SCK-NPs with super high specific activity (radioactivity over mass), which will make the study of targets with low density possible. This project can be used for imaging (e.g. cancer) and target therapy.

2. A comparison of the actual accomplishments with the goals and objectives of the project

Goals and objectives of the project	Accomplishments
I.A. Prepare moieties for radiolabeling with Cu-64 and F-18	Several moieties for Cu(I) catalyzed and Cu-free click labeling have been synthesized, and some of them have been labeled with Cu-64 or F-18.
I.B. Prepare SCK-NPs with azide and alkyne groups in core and shell	SCK-NPs with different % of azide and alkyne groups in core and shell or in shell and core have been prepared.
II.A. Radiolabel SCK-NPs with Cu-64 and F-18 indirectly by Click chemistry	Cu(I) catalyzed click labeling was first attempted with little success. Cu-free click labeling has been successfully applied to label SCK-NPs with Cu-64 and F-18.
II.B. Specific activity determination and autoradiolysis studies on Cu-64 and F-18 labeled SCK-NPs	Ultra high specific activity has been achieved with Cu-64 labeling of SCK-NPs using Cu-free moiety. No autoradiolysis has been done due to time limit.
II.C. <i>In vivo</i> PET & biodistribution of Cu-64 and F-18 radiolabeled SCK-NPs	This has not been done due to the <i>in vivo</i> studies to establish an animal model for CA12.
III.A. Prepare azide and alkyne-substituted ligands for CA12	Two CA general ligands and two CA12 specific ligands have been made. And they have been labeled with Cu-64 and F-18 using click chemistry.
III.B. Prepare CA12-targeted Cu-64 and F-18 labeled SCK-NPs and characterize their CA12 binding <i>in vitro</i> and in cells	A CA12 specific ligand has been labeled with F-18, and <i>in vivo</i> animal studies have been done in order to establish an animal model of CA12 and for comparison with CA12-target SCK-NPs.
III.C. <i>In Vivo</i> PET & Biodistribution of Cu-64 and F-18 Radiolabeled SCK-NPs Targeted to CA12	

3. Introduction

Nuclear imaging techniques (PET and SPECT) are widely used in medicine for the diagnosis of a wide variety of vascular, pulmonary, and metabolic pathologies, and for identifying, staging, and characterizing various cancers. A great advantage of PET and SPECT is the fact that very high specific activity radiopharmaceuticals can be prepared and used to detect low abundance biomarkers. Currently, the vast preponderance of PET and SPECT radiopharmaceuticals are based on small molecules. While many of these perform satisfactorily, their small size limits their functional characteristics. By contrast, nanoparticles, which are larger and more diverse in size, shape and composition, have multi-valent and potentially unique multi-functional character, and over the last several years, there have been many publications on the use of nanoparticles as both imaging (1-4) and therapeutic agents (5,6). One important drawback in using nanoparticles for nuclear imaging, however, is that when they are prepared by currently available procedures, only a few radioactive atoms can be attached to a single nanoparticle; thus, the amount of radioactivity per mass of agent is relatively low. Also, the stability of labeled nanoparticles towards autoradiolytic damage is not known.

4. Background

The nanoparticles to be used in this project are shell crosslinked knedel-like nanoparticles (SCK-NPs, or SCKs for short), unique molecular entities developed in the laboratory of one of the Co-Principal Investigators, Karen Wooley. SCK-NPs have controllable size, shape, flexibility, and functionality, and because of the manner in which they are prepared and their distinctive core-shell structure, SCK-NPs offer unique opportunities for achieving the very high specific activity and effective molecular targeting activity required for the detection and quantification of low abundance biological targets using nuclear imaging. Dr. Wooley and Dr. Michael J. Welch, the Principal Investigator, have worked together on SCK-NPs targeted to the folate receptor system, and they have developed a good understanding of the structure-activity relationships for controlling clearance in blood and interactions with biological targets in cancer (1,2).

In this project, highly efficient Click chemistry methods will be developed to label specifically the core vs. the shell of SCK-NPs in an orthogonal and efficient

fashion, with both radiotracer and molecular targeting moieties. Dr. Wooley has expertise with Click chemistry (7-9), and she will use azide and alkyne-substituted tracer moieties, labeled with Cu-64 or F-18, and targeting ligands, developed by the other Co-Principal Investigator, Dr. John Katzenellenbogen, to substitute the SCK-NPs. Because they are spatially separated, the azide and alkyne groups in the core and shell regions of the SCK-NPs will not react with one another. Also, because the labeling is a two-step, indirect process, it is anticipated that much more efficient and higher levels of labeling will be attainable. The number, nature, and placement of the radiotracer and CA12-targeting ligands on the SCK-NPs will be varied to optimize specific activity, autoradiolytic stability, and CA12 targeting efficiency. Specific interaction of these novel SCK-NPs with the CA12 will be ascertained in breast cancer cells, and in vivo μ PET imaging of CA12 in animal models of breast cancer will be done under the direction of Dr. Welch.

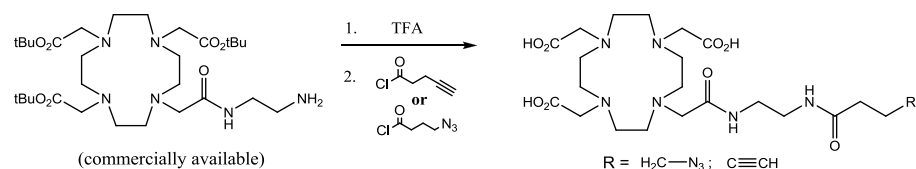
5. Results

5.1. Preparation of Radiolabeling Moieties: Synthesis of Azide- and Alkyne-Substituted Molecules for Two-Step Radiolabeling of SCK-NPs with Cu-64 and F-18 by Click Chemistry

5.1.1. Introduction

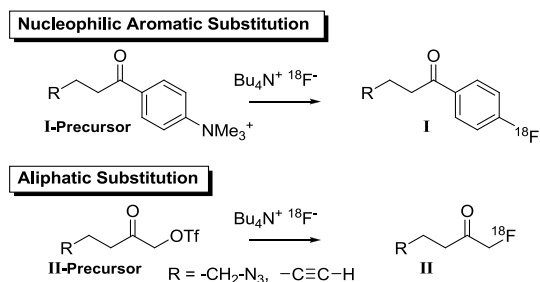
The key limitations of the pre-conjugation of ligands onto the block copolymers prior to their assembly into SCK nanoparticles are that new particles must be assembled from each new polymer composition, the ligands attached can alter the size and shape of the particles, and direct pre-attachment of radioactivity cannot be done because of the time and conditions required for the micellar assembly, shell crosslinking and purification of the particles. The alteration of particle morphology (size and shape) becomes a significant problem as the number of perturbing (DOTA) ligands increases. We will need the efficiency of Click chemistry to be able to introduce the desired maximum number of radiolabels into the final SCK nanoparticle.

Moieties for labeling with Cu-64 — Examples of azide- and alkyne-substituted copper chelates suitable for attachment to SCK-NPs by Click chemistry are shown in Scheme 1.



Scheme 1. Proposed synthesis of DOTA derivatives for Cu-64 labeling of SCK-NPs by Click chemistry.

Moieties for labeling with F-18 — To label SCK-NPs with F-18, we will investigate two chemistries for the preparation of F-18-bearing small molecules that also contain an alkyne or azide functionality: nucleophilic aromatic substitution and aliphatic substitution (Scheme 2).

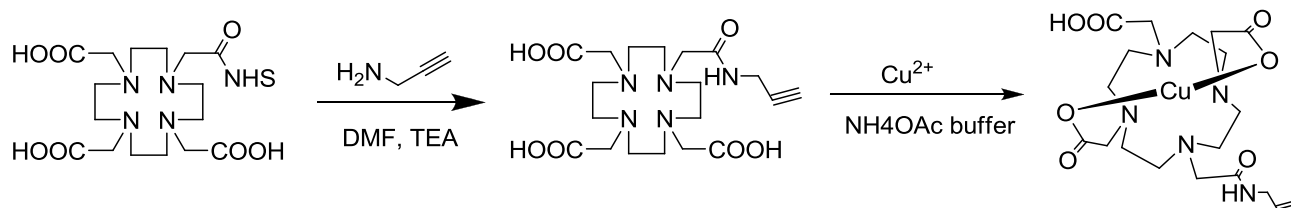


Scheme 2. Proposed F-18 radiolabeling of azide and alkyne derivatives for labeling of SCK-NPs by click chemistry.

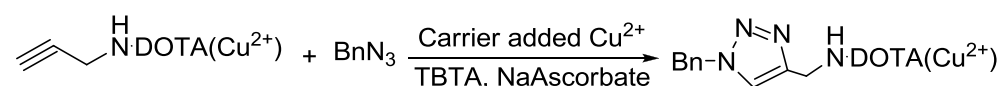
5.1.2. Results

5.1.2.1. Synthesis of DOTA-alkyne derivative for Cu(I) catalyzed click labeling

A DOTA-alkyne derivative has been synthesized and labeled with Cu-64 according to Scheme 3. The Cu-64 labeled DOTA-alkyne derivative has been tested with model compound under typical Cu(I) catalyzed click conditions, significant copper exchange has been observed (Table 1). This observation let us seek for copper-free click chemistry.



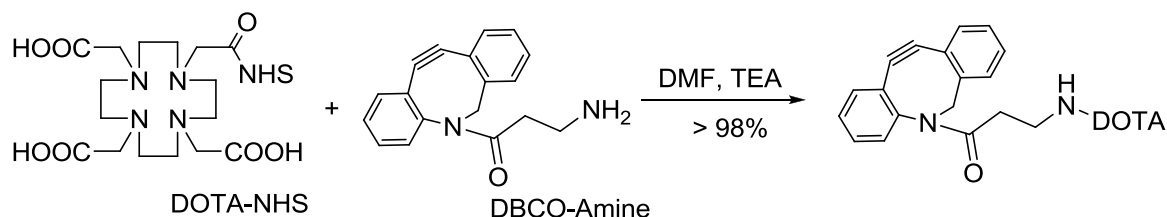
Scheme 3. Synthesis and radiolabeling with Cu-64 of DOTA derivative

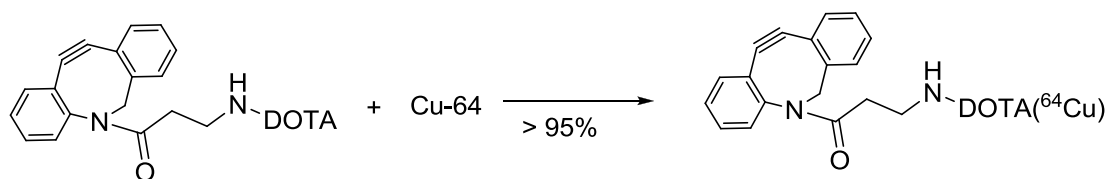
Table 1. Model labeling reaction using Cu(I) catalyzed click chemistry

		“Click” reaction	Control
DOTA-alkyne- ⁶⁴ Cu		1.0 eqv.	1.0 eqv.
TBTA + Cu (I) (as carrier)		1.0 eqv.	1.0 eqv.
BnN ₃		1.0 eqv.	None
Extent of reaction (%)		> 90	N/A
distribution of Cu-64 (%)	Free	88.52	97.27
	in DOTA-Alkyne	3.06	2.73
	in click Product	8.42	N/A

5.1.2.2. Synthesis of DOTA-DBCO derivative for Cu-free click labeling

The DOTA conjugated DBCO (dibenzocyclooctyne) was synthesized from DOTA-NHS ester and DBCO primary amine derivative, and then was purified by HPLC and used for the subsequent chelating experiments (Scheme 4). After the Cu-64 ammonia acetate buffer solution was incubated with a large excess (~50 folds) of DBCO-DOTA at 37 °C for 30 minutes, usually over 80% radiolabeling yield could be obtained. The excess chelator could be separated from the copper complex by HPLC (Figure 1). Impressively, under the optimized condition, besides the excess chelator, the complexes with other transition metals (Fe³⁺, Ni²⁺, Zn²⁺, Co²⁺) that was already existed in the cyclotron produced Cu-64 could also be separated (or partially separated) from the Cu-64 complex.





Scheme 4. Synthesis of DBCO-DOTA and Cu-64 radiolabeling of DBCO-DOTA.

Copper-free click reagent, DBCO (dibenzocyclooctyne)

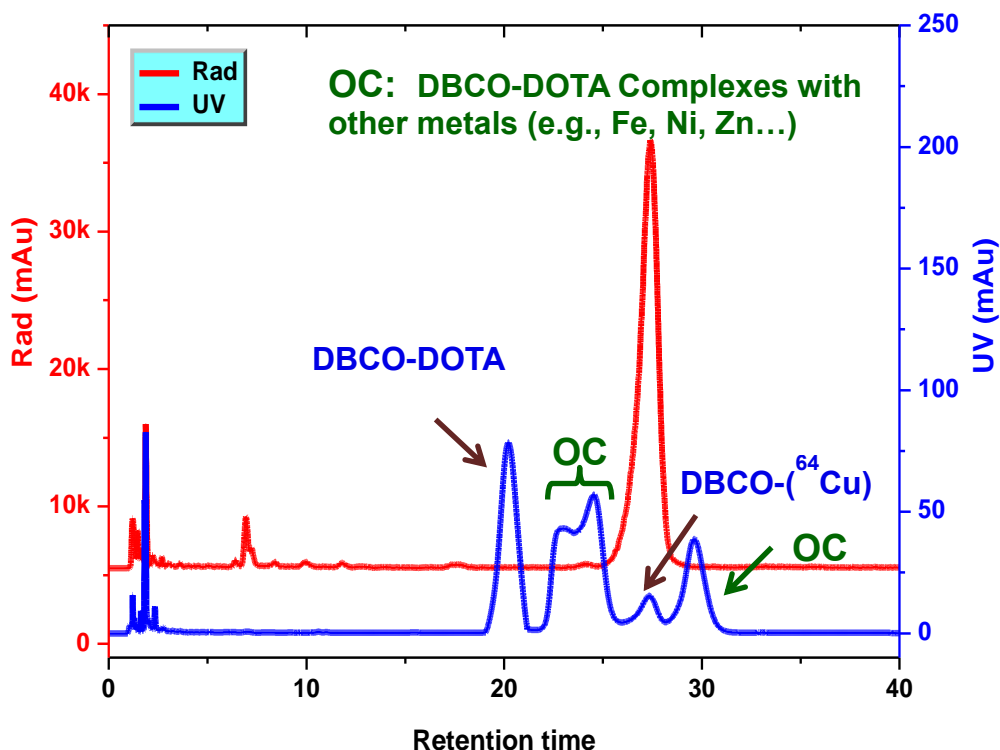
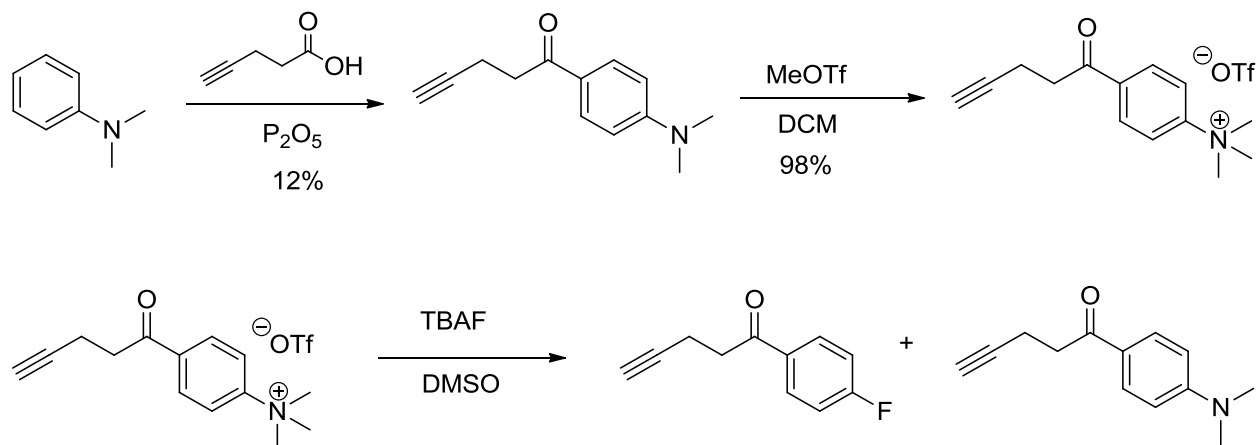


Figure 1. HPLC chromatograph of DBCO-DOTA- ^{64}Cu complex

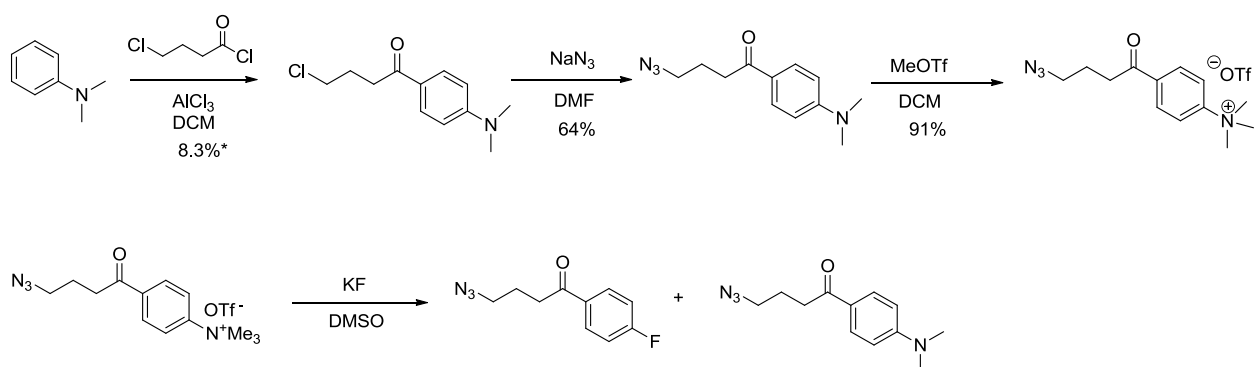
5.1.2.3. Synthesis of alkyne and azide derivative for F-18 labeling of SCK-NPs using Cu(I) catalyzed click chemistry

Two precursors for aromatic nucleophilic substitution method (trimethyl-(4-pent-4-ynoyl-phenyl)-ammonium triflate and [4-(4-Azido-buteryl)-phenyl]-trimethyl-ammonium triflate) and their reference compounds have been synthesized according to Scheme 5.

Acetylene-Adaptor

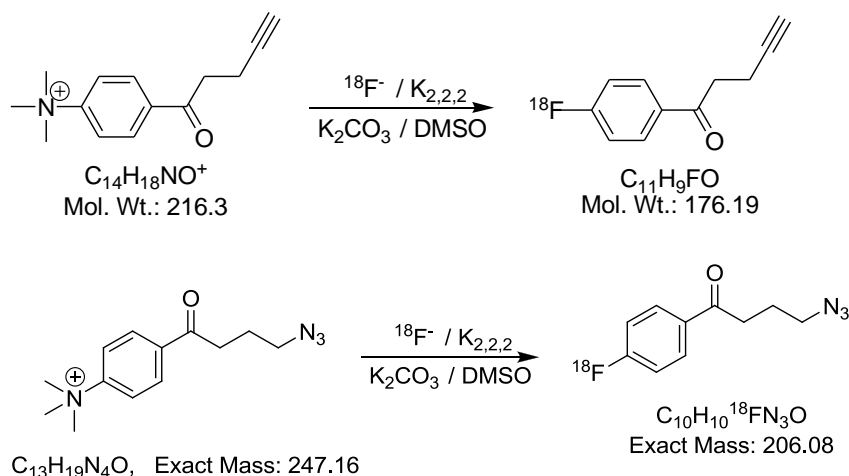


Azide-Adaptor



Scheme 5. Synthesis of precursors and references for F-18 labeling of alkyne and azide derivatives for click labeling of SCK-NPs.

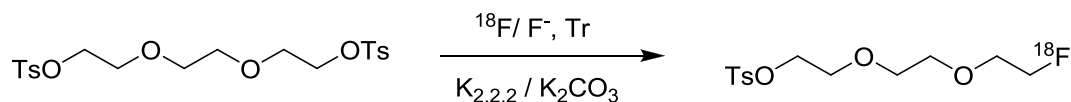
The alkyne moiety has been labeled with F-18 using aromatic nucleophilic substitution to afford the alkyne derivative in good radiochemical purity and yield after reversed phase HPLC purification. This compound has been used to optimize the click labeling condition with SCK-NPs. The azide moiety has been attempted using same method. However, under the conditions that incorporation of F-18 were observed, the major radiolabeled product was not the desired product, and this product underwent no click reaction.

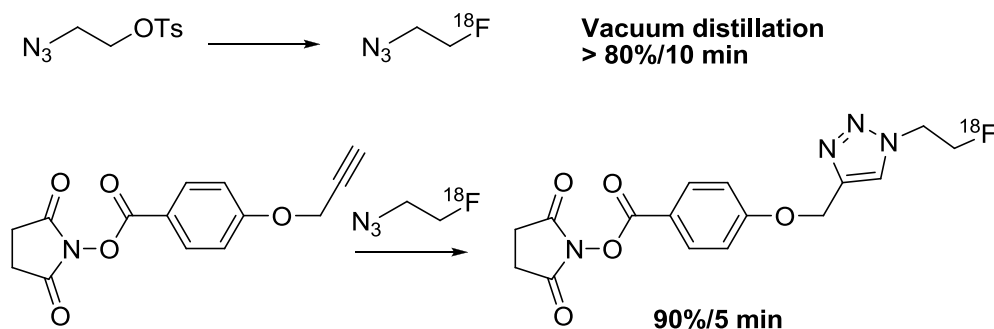


Scheme 6. Radiosynthesis of alkyne moiety and attempted radiosynthesis of azide moiety using aromatic nucleophilic substitution.

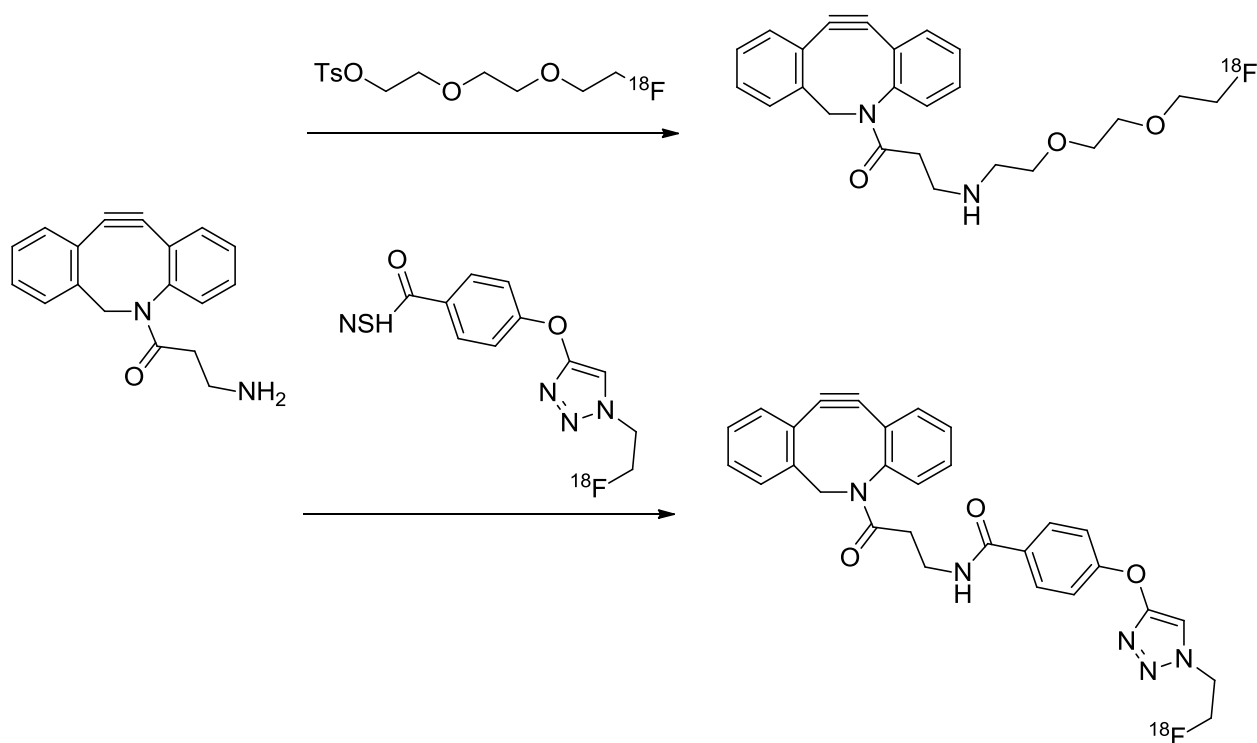
5.1.2.4. Synthesis of DBCO derivative for F-18 labeling of SCK-NPs using Copper-free click chemistry

Two DBCO derivatives have been radiolabeled with F-18 using two F-18 labeled prosthetic compounds, which are shown in Scheme 7. The PEG was used to improve the water solubility of DBCO derivative. However, this route afforded variable yields, from poor to good. A new NHS ester has been developed using click labeling with 2-[F-18]fluoroethyl azide (Scheme 7). The F-18 labeled NHS ester provided a more efficient conjugation with DBCO-NH₂ with improved water solubility of DBCO (Scheme 8). Both DBCO derivatives have been used to study the radiolabeling of SCK-NPs using copper-free method.





Scheme 7. Radiosynthesis of prosthetic compounds for conjugation with DBCO-NH₂



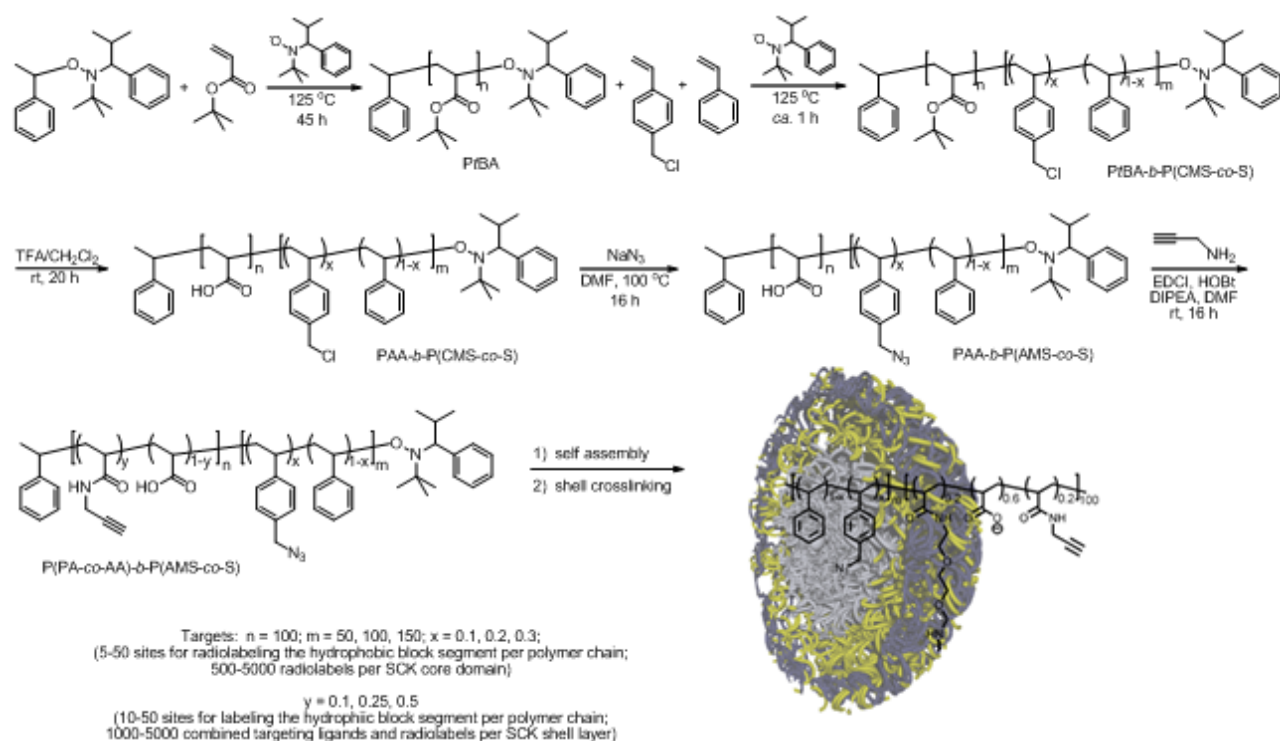
Scheme 8. Radiolabeling of DBCO derivatives with F-18

5.2. Preparation of SCK-NPs Having Alkynes in the Shell and Azides in the Core, Each Available for Complementary, Orthogonal Click Chemistry Reactions.

5.2.1. Introduction

As outlined in **Scheme 9**, azides and alkynes can each be introduced as side chain substituents along an amphiphilic block copolymer, which then places those

groups into different domains within SCK nanoparticles. Nitroxide-mediated radical polymerization will be used to establish first a homopolymer of *tert*-butyl acrylate (PtBA) and then extension into a block copolymer of *tert*-butyl acrylate and styrene containing repeat units also of chloromethyl styrene (PtBA-*b*-PCMS-*co*-S). Removal of the *tert*-butyl ester protecting groups will then afford an amphiphilic block copolymer of acrylic acid and styrene copolymerized with chloromethyl styrene. We have already developed this chemistry to produce these block copolymers as well defined structures (10), having control over the absolute and relative lengths of the acrylic acid and styrene-*co*-chloromethyl styrene block segment lengths and also over the amount of chloromethyl styrene incorporated. The hydrophilic:hydrophobic chain length ratio and overall polymer length determine the size of the micelles and subsequent SCKs that will result. The amount of chloromethyl styrene will determine the number of azide groups that are introduced by reaction with sodium azide. The number of alkynes can also be controlled by the degree of amidation of the acrylic acid residues upon reaction with propargyl amine.

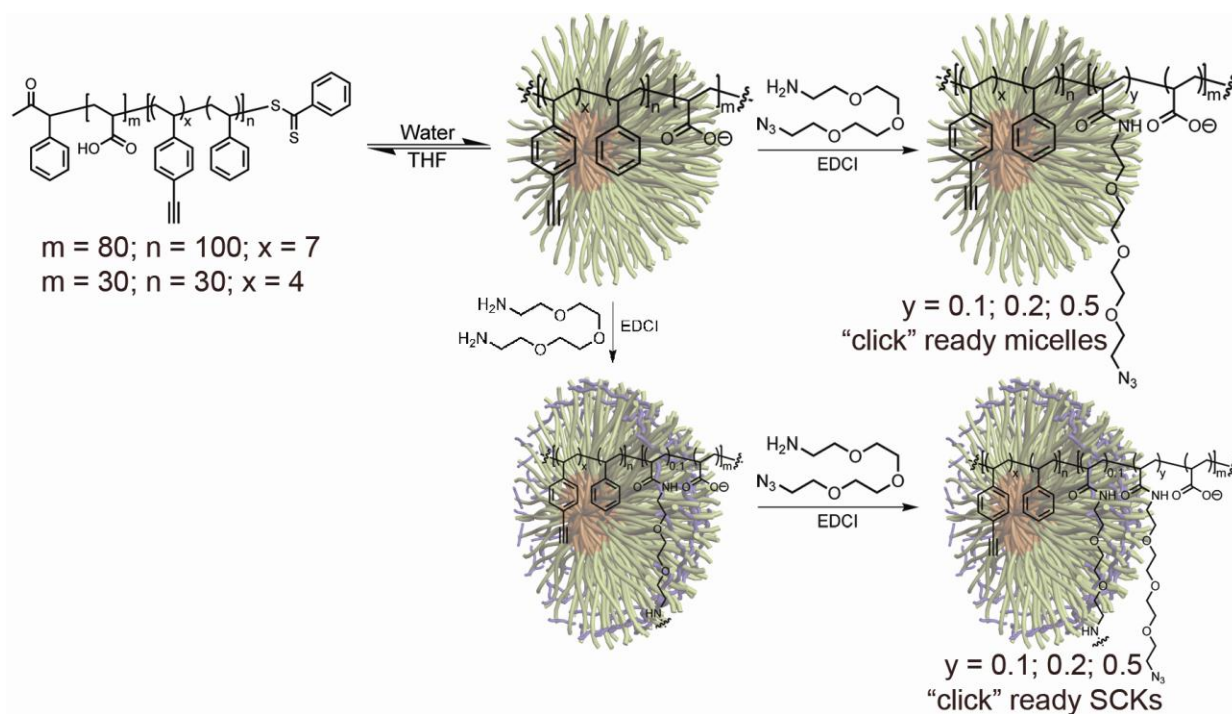


Scheme 9. Proposed synthesis of SCK-NPs with azide/alkyne in the core and shell.

5.2.2. Results

5.2.2.1. Synthesis of SCK-NPs with alkyne in the core and azide in the shell.

12 micelles and SCKs were prepared (Scheme 10) with different core/shell sizes, acetylene contents in the core, and azide contents in the shell (Table 2). A TEM image of a micelle is also shown in Figure 2.



Scheme 10. Preparation of core/shell "click" ready micelles and SCK-NPs.

Table 2. Summary of "click" ready micelles and SCKs with varying contents of acetylenes (x) and azides (y).

	Micelle (SS- <i>i</i> -24; SS- <i>i</i> -23)						SCK (SS- <i>i</i> -26; SS- <i>i</i> -25)					
	1A	1B	1C	2A	2B	2C	1A	1B	2C	1A	1B	2C
m	30			80			30			80		
n	30			100			30			100		
x	4			7			4			7		
y	10%	20%	50%	10%	20%	50%	10%	20%	50%	10%	20%	50%

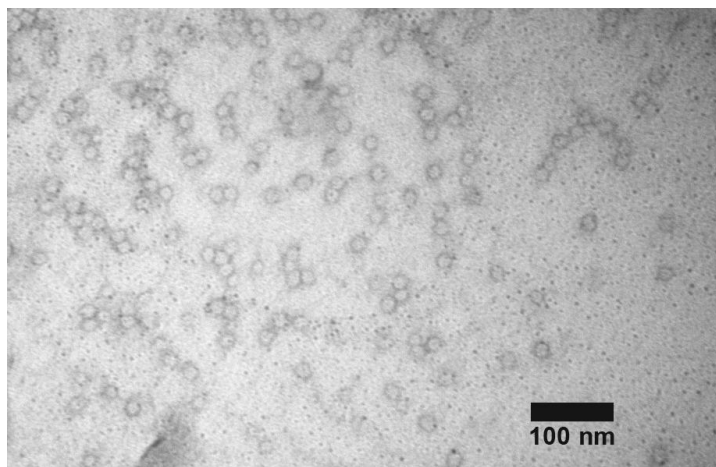


Figure 2. Transmission electron microscopy image of Micelle 1C.

5.2.2.2. Click labeling in the core of micelles or SCK-NPs

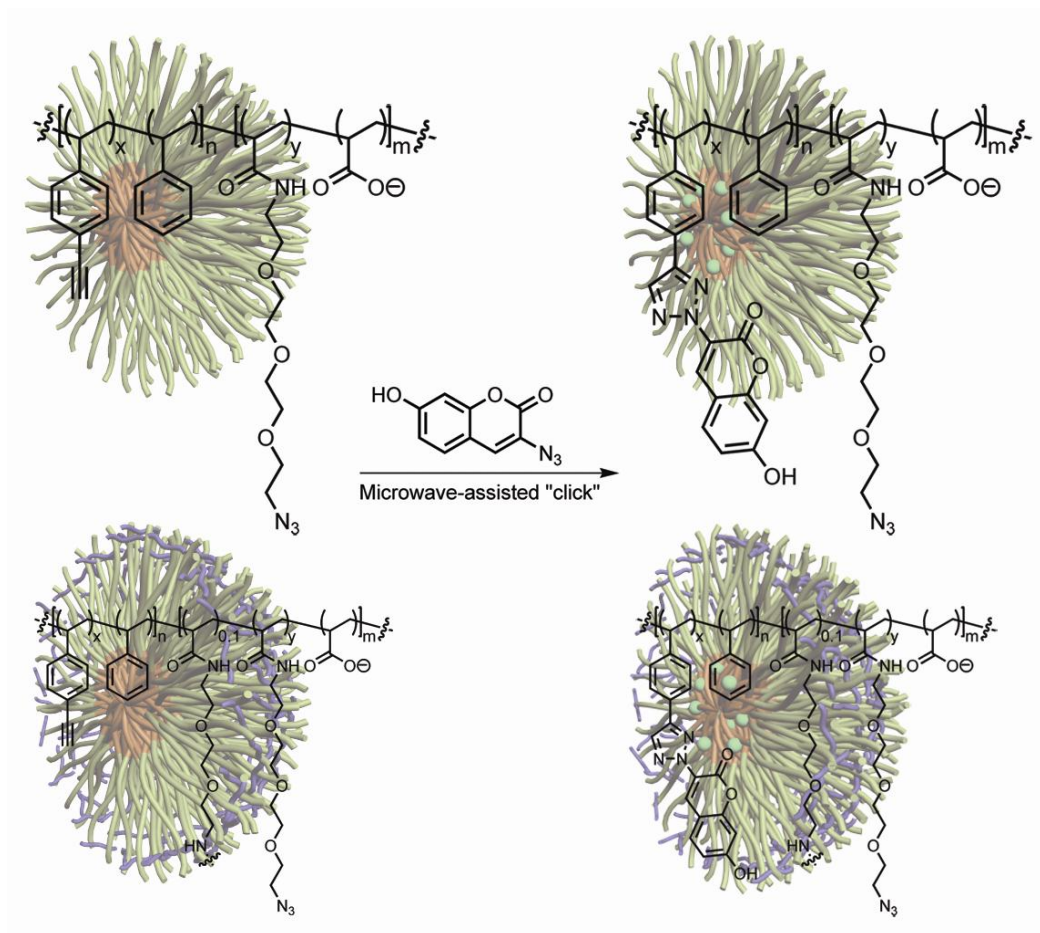


Figure 3. Microwave-assisted “click” reactions of 3-azidocoumarin onto the core of the micelles or SCK-NPs

The core/shell functionalization of micelles or SCK-NPs has been demonstrated by microwave-assisted click reaction of micelles or SCK-NPs with 3-azidocoumarin in the presence of $\text{CuSO}_4 \cdot 5\text{H}_2\text{O}$, and Na ascorbate dissolved in DMF. The reaction mixture was subjected to the microwave conditions summarized in Table 3. Fluorescence emission spectra were collected immediately before and immediately after conducting the microwave reactions.

Upon adding all the reagents to the micelle or SCK solutions, fluorescence emission spectra were collected (blue curve) to reveal no significant fluorescence emission. However, after the microwave reactions, all 12 samples showed intense fluorescence emission confirming 3-azidocoumarin's pre-fluorophore nature (Figure 4). We have demonstrated successful core "click" reactions of 3-azidocoumarin and acetylene-containing core residues of micelles and SCKs through rapid microwave reactions.

Table 3. Microwave conditions employed and pressures reached for core "click" reactions.

	Micelle (SS-i-24; SS-i-23)						SCK (SS-i-26; SS-i-25)					
	1A	1B	1C	2A	2B	2C	1A	1B	1C	2A	2B	2C
Duration (min)	10	7	7	6	7	10	10	8	10	7	8	7
Pressure (bar)	7	22	22	22	22	22	13	22	7	22	22	22
Power	100 W											
Temp	40 °C											

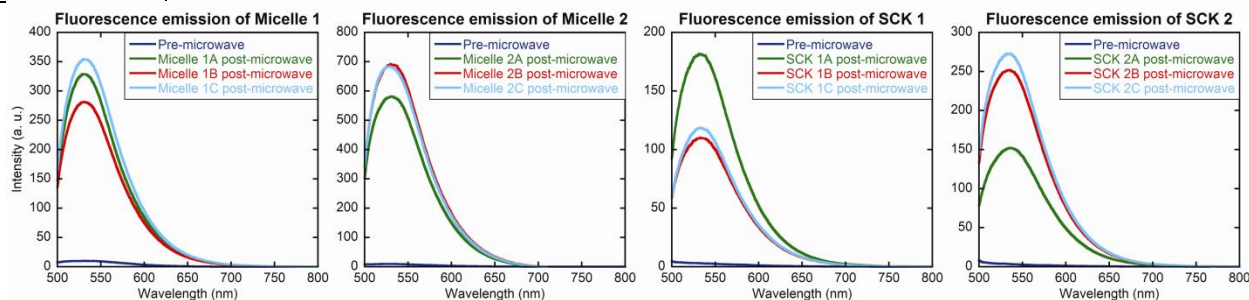


Figure 4. Fluorescence emission of micelles and SCKs before and after the microwave-assisted "click" reaction ($\lambda_{\text{ex}} = 488 \text{ nm}$).

5.2.2.3. Synthesis of SCK-NPs with azide in the core and alkyne in the shell

SCK-NPs with various amounts of azide in the core and alkyne in the shell have been synthesized as shown in Figure 5. A representative TEM image of a click-ready SCK and a representative DLS histogram of a click-ready SCK-NPs are shown in Figure 6.

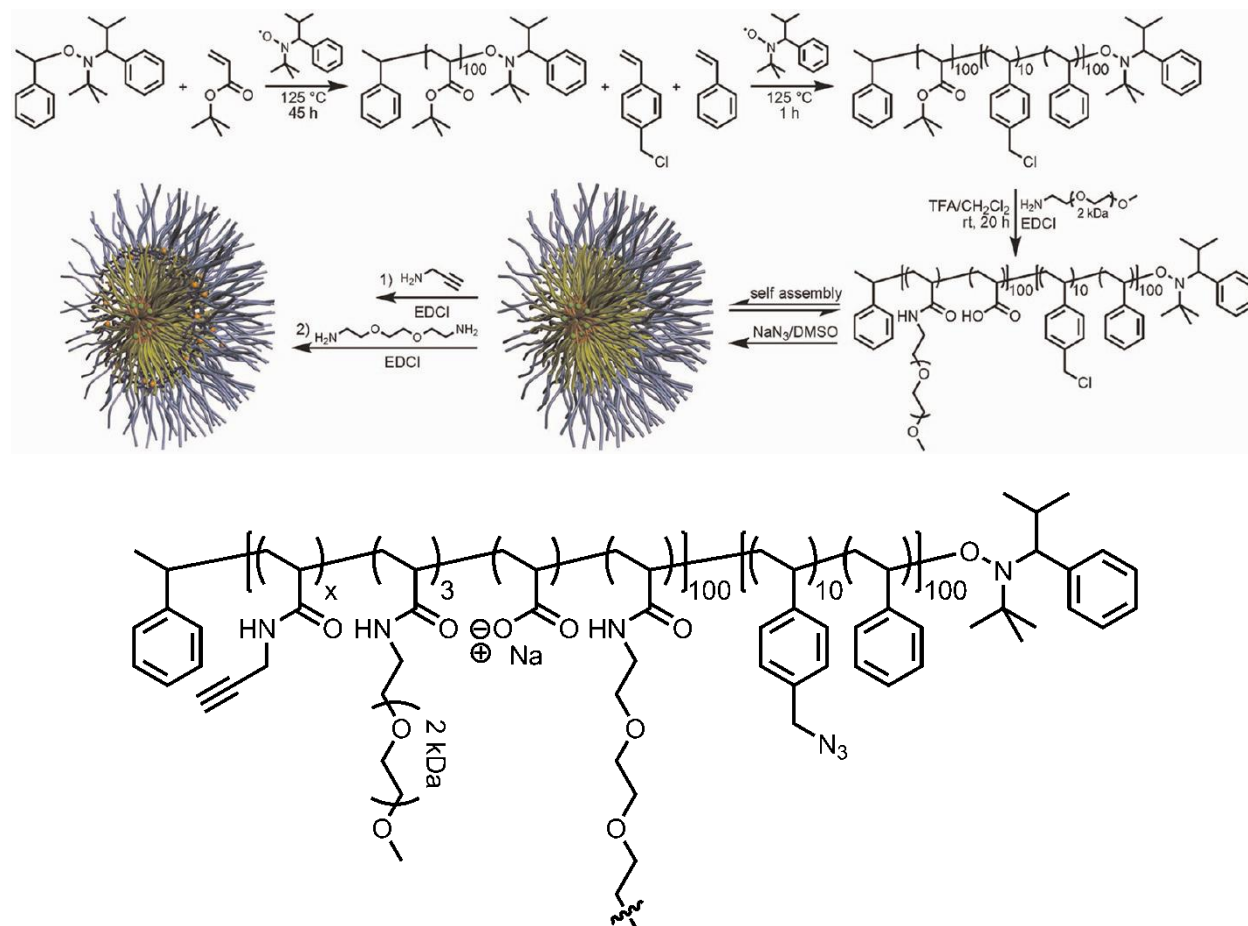


Figure 5. Synthesis of SCK-NPs-containing azides in the core and alkynes in the shell and a typical chemical structure

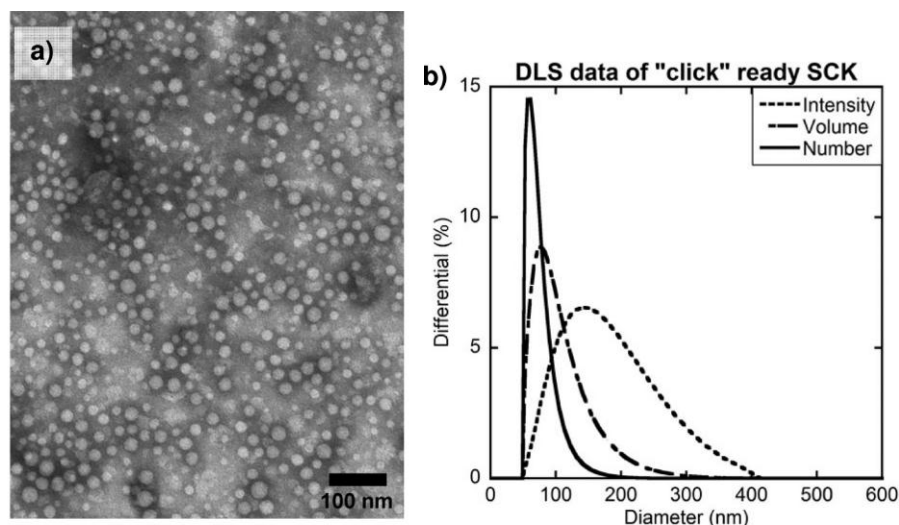


Figure 6. (a) Representative TEM image of a click-ready SCK (average diameter = 22 ± 2 nm). (b) Representative DLS histogram of a click-ready SCK ($D_{\text{int}} = 120 \pm 35$ nm, $D_{\text{vol}} = 95 \pm 15$ nm, $D_{\text{num}} = 65 \pm 5$ nm).

Table 4. Summary of SCK-NPs with various amounts of alkyne in the core and azide in the shell

micelle	azide contents $y = 10\%$	10% Xlink SCK	azide contents $y = 10\%$
acetylene contents $x = 5\%$	NL-iv-31A 0.62 mg/mL	acetylene contents $x = 5\%$	NL-iv-32A 0.55 mg/mL
acetylene contents $x = 20\%$	NL-iv-31B 0.60 mg/mL	acetylene contents $x = 20\%$	NL-iv-32B 0.53 mg/mL
acetylene contents $x = 50\%$	NL-iv-31C 0.54 mg/mL	acetylene contents $x = 50\%$	NL-iv-32C 0.49 mg/mL

Note: NL-iv-32B: Acetylene contents of 20% refers to the amount of acetylene functionalities with respect to the PAA repeat units of 100, where x would equal to 20. The molar amount of acetylene functionalities, then, can be calculated by dividing the mass of the polymer (use concentration of 0.53 mg/mL) by 24.2 kDa and multiplying the quotient by 20 (*i.e.*, for 1 mL of NL-iv-32B, there is 0.438 mmol of acetylenes)

5.3. Preparation of the Cu-64 and F-18 Radiolabeling Moieties and Their Attachment Specifically in the Core or on the Shell of SCK-NPs Using Click Chemistry

5.3.1. Introduction

We will use the specificity and high efficiency of Click chemistry in optimizing the level of SCK-NP radiolabeling, to achieve the highest possible specific activity with Cu-64 and F-18.

Preparation of the Cu-64 and F-18 radiolabeled precursor moieties — For step 1 of these radiolabeling studies, the different Cu-64 complexes and F-18 labeled moieties designed for click chemistry will be prepared. This will involve reaction of the chelates with Cu-64 in ammonium hydroxide buffer and purification by ion exchange. Labeling with F-18 will involve reaction of an excess of the labeling precursors with F-18 fluoride. To remove the excess, unreacted precursor, the F-18 labeled moiety will be purified by HPLC or passing through a silica gel SepPak.

Attachment of the Cu-64 and F-18 radiolabeled precursor moieties to the SCK-NPs by Click chemistry — This is a critical aspect of our work and will involve comparisons of conditions and approaches that are to be evaluated in terms of NP labeling efficiency and NP specific activity:

- Varying the quantities of SCK relative to the Cu-64 and F-18 radiolabeled moieties and optimizing the time, concentrations, and the nature and amount of the copper catalyst.
- Comparing Click chemistry with NP-azide vs. NP-acetylene groups.
- Comparing introduction of radiolabel in the core vs. the shell of the SCK.
- Comparing the radioisotopes copper-64 and fluorine-18.

Because it is not feasible to separate radiolabeled NPs from unlabeled ones, the only way we have for preparing high specific activity NPs is by optimizing the radiolabeling reaction conditions. In this regard, we expect that as the quantity of SCK-NP is decreased relative to the radiolabeling moiety, labeling efficiency (i.e., overall consumption of the radiolabel) will decrease but specific activity (i.e., radioactivity per NP) will increase. After the Click chemistry to attach the labeled

moieties, the labeled NPs will be separated from any unreacted radiolabeling moiety by HPLC.

The key to obtaining high specific activity lies in the Click chemistry reaction efficiency (20). We will explore the effect of NP concentration, Cu(I) catalyst, and reaction times and conditions to achieve the highest efficiency for Click chemistry. Regarding time, we will have more leeway with Cu-64 ($t_{1/2} = 12.9$ h) than with C-18 ($t_{1/2} = 110$ min). While it is not clear that one would be preferable to the other, we will see which coupling strategy—acetylene labeling moieties to NP-azides, or azide labeling moieties to NP-acetylenes—gives higher specific activities.

It is difficult to predict whether introducing the radiolabel in the core or on the shell of the SCK will be preferable in terms of attainable specific activity or labeling efficiency, although the reaction in the shell might be more rapid. The location of the radionuclide might have a larger effect on autoradiolytic stability. Other than the permissible reaction times, noted above, there might be significant differences in the efficiency with which the Cu-64 and the F-18 labeling moieties react with the SCK-NPs because of the different chemical nature of the labeling moieties required to secure the radiolabel.

Estimation of the specific activity of the Cu-64 and F-18 radiolabeled SCK-NPs — While it is simple to determine labeling efficiency, it is more challenging to determine the specific activity of radiolabeled NPs than radiolabeled small molecules. We believe that this can be done, however, because it is possible to determine the number of SCK-NP present in a volume of solution. If this volume of NPs reacts with the labeling moiety with a certain efficiency (determined after removal of all unreacted labeling moiety), then one also knows the amount of radioactivity associated with the NP. Thus, by knowing the incorporated activity and the quantity of NPs, one can calculate specific activity and the number of radionuclides associated with each NP. While there might be inaccuracies in determining NP specific activity, it should not be difficult to determine relative specific activities and use these values in optimizing radiolabeling conditions.

5.3.2. Results

5.3.2.1. Preparation of the Cu-64 and F-18 radiolabeled precursor moieties

Alkyne and azide moieties for Cu(I) catalyzed and copper-free click chemistry have been labeled with Cu-64 and F-18 as reported above.

5.3.2.2. Attachment of the Cu-64 and F-18 radiolabeled precursor moieties to the SCK-NPs by Click chemistry

5.3.2.2.1. Stability of SCK-NPs under condition of Cu(I) catalyzed click chemistry

The stability/compatibilities of SCK-NPs towards Cu(I) catalyzed click chemistry has been investigated, and the results are shown in Table 5 and 6. The results suggest that the NL-iV-32B SCK-NPs should be compatible with the “click chemistry” at elevated temperature (60 °C). However, the SS-i-10A SCK-NPs was not good with the “click chemistry” at elevated temperature (60 °C).

Table 5. Stability of SCK-NPs towards Cu(I) catalyzed click chemistry

	Azide in core, SCK NPS				Acetylene in Core, SCK NPS	
NPS #	NL-iV-32A	NL-iV-32B	NL-iV-32C	NL-iV-22B	SS-i-9A	SS-i-10A
NPS itself, 23 °C ¹	OK	OK	OK	Fully degraded	OK	OK
No NaAscorbate, 23 °C ²	OK	OK	OK	-	OK	OK
No NaAscorbate, 60 °C ³	OK	OK	OK	-	Partially degraded	Partially degraded
With NaAscorbate ⁴	OK	OK	OK	-	Fully degraded	Fully degraded
“click” compatibilities	Good	Good	Good	-	No	No

Table 6. FPLC analysis of SCK-NPs under Cu(I) catalyzed click conditions

	NPS	Pre-swell solvent	Catalysis	NaN ₃	Sodium Ascorbate	Temperature	Reaction time	Mass (UV, mAu)		Note
								NPS @ 7.9 mins	Peaks after 16.5 mins (small molecules)	
1	NL-iV-32B	H ₂ O	H ₂ O	H ₂ O	H ₂ O	23 °C	30	13.5	N/A	
2	NL-iV-32B	H ₂ O	H ₂ O	H ₂ O	H ₂ O	60 °C	30	8.5	N/A	
3	H ₂ O	H ₂ O	50% DMSO	H ₂ O	H ₂ O	23 °C	30	N/A	1 peaks	
4	NL-iV-32B	H ₂ O	50% DMSO	H ₂ O	H ₂ O	23 °C	30	13.0	1 peaks	
5	NL-iV-32B	DMF	50% DMSO	H ₂ O	H ₂ O	60 °C	30	14.25	1 broad peaks	
6	NL-iV-32B	DMF	Cu(II)-TBTA	NaN ₃	H ₂ O	60 °C	30	7.5	4 peaks	
7	NL-iV-32B	DMF	Cu(II)-TBTA	NaN ₃	Na Ascorbate	60 °C	30	13.5	5 peaks	
8	NL-iV-32B	DMF	Cu(II)-TBTA	NaN ₃	Na Ascorbate	60 °C	60	11.5	5 peaks	
9	SS-i-10A	DMF	Cu(II)-TBTA	NaN ₃	Na Ascorbate	60 °C	30	No peak	6 peaks	New peak at 21.00 mins
10	SS-i-10A	H ₂ O	H ₂ O	H ₂ O	H ₂ O	23 °C	30	35	N/A	

5.3.2.2.2. Radiolabeling of SCK-NPs with F-18 labeled alkyne moiety

Cu(I) catalyzed labeling of SCK-NPs using F-18 labeled alkyne has been investigated. The results are shown in Table 7 and Table 8. Up to 25 % yield was obtained under a variety of conditions.

Table 7. Click labeling of SCK-NPs

Solvent	Azide	Time (min)	% of activity on TLC origin	Click yield (%) ₁	Note
NO	NL-ii-102 no azide, no acetylene	30	7%	N/A	blank
		60	7%	N/A	
		90	4%	N/A	
	NL-ii-90A 10% azide in core, 20% acetylene on shell	30	6%	0	
		60	6%	0	
		90	6%	2%	
	SS-ii-10B 7% acetylene in core, 20% azide on shell	30	10%	3%	
		60	16%	9%	
		90	15%	11%	
	SS-ii-10B No NaAscorbate 7% acetylene in core, 20% azide on shell	30	0	0	
		60	0	0	
		90	0	0	
50 μ L of DMF	NL-ii-102 no azide, no acetylene	15	7%	N/A	blank
		30	7%	N/A	
		60	7%	N/A	
	NL-ii-90A 10% azide in core, 20% acetylene on shell	15	28%	21%	
		30	30%	23%	
		60	32%	25%	
50 μ L DMF and 50 of alcohol	NL-ii-90A 10% azide in core, 20% acetylene on shell	15	28%	21%	
		30	25%	18%	
		60	25%	18%	
	No NPS ²	15	13%	N/A	Activity decomposed
		30	8%		
		60	12%		

Click procedure:

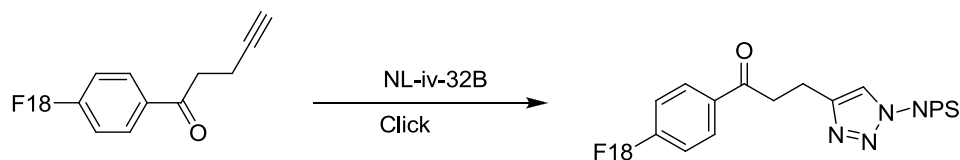
1. 50 μ L 0.53 mg/mL NL-ii-90A (or NL-ii-102, or SS-i-10B) solution was added to 1.70 mL eppendorf tube.
2. 50 or no μ L DMF or alcohol was added to previously swell the above NPS.

3. 40 μL 5 mM Cu(II)-TBTA (1 : 1) 50% DMSO aqueous solution was added to above eppendrof tube, followed by 100 μL R-F18 solution we previously prepared.
4. 5 or 0 μL of 50 mM sodium ascorbate aqueous solution was added to initial the “click” reaction.
5. The above mixture was incubated for 30 or 60 or 90 minutes at 50 $^{\circ}\text{C}$, and then was analyzed by radio-TLC:

Table 8. Comparison of Click labeling of SCK-NPs using heating and microwave

Condition Sample #	Catalysis, 5mM	Na ascorbate 10 mM	Heating (@ $^{\circ}\text{C}$)	Reaction time	% of activity (on the bottom)
1	10 μL Cu(II)	10 μL	Convention(40)	30	0
2	10 μL Cu(II)- TBTA	10 μL	Microwave(40)	10	0
3	10 μL Cu(II)- TBTA	10 μL	Microwave(60)	10	~ 3
4	50 μL Cu(II)- TBTA	100 μL	Microwave(60)	10	~ 10
5	50 μL Cu(II)- TBTA	100 μL	Convention(60)	30	~ 5
6	40 μL Cu(II)- BPDS	100 μL	Convention(60)	30	~ 10
7	40 μL Cu(II)- BPDS	100μL	Microwave(60)	10	~ 25

The scheme of a typical “click” reaction is shown in scheme 11), and the results obtained from conventional way and biotage microwave have been compared. Their incorporated yields are 10% and 25%, respectively (Table 8). After SEC purification, on FPLC spectrum (Figure 7), the retention time of the radiation peak was same as that of UV peak, which suggested that the F-18 labeled acetylene clicked with SCKs.



Scheme 11. The click reaction between F-18 labeled acetylene and SCK-NP.

However, a significant radio activity shift was observed when the fully developed radio-TLC plate of SEC purified product (Figure 8) was re-developed twice, which indicated that the F-18 labeled acetylene had significantly been wrapped/dissolved (not covalently) in the SCKs under the Cu(I) catalyst “click” condition. This observation led up to look for copper-free click labeling.

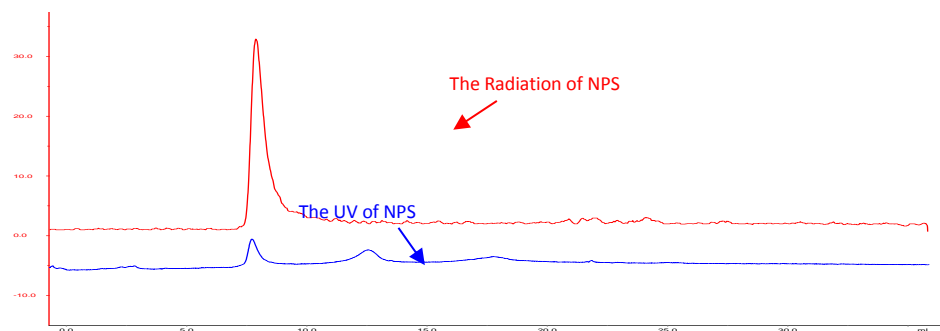


Figure 7. FPLC chromatograph of F-18 labeled SCK-NP

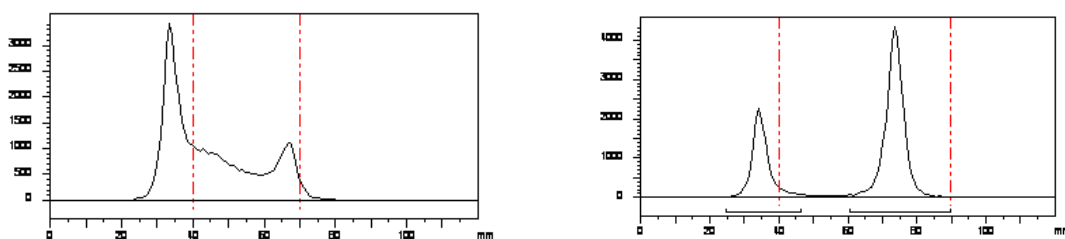
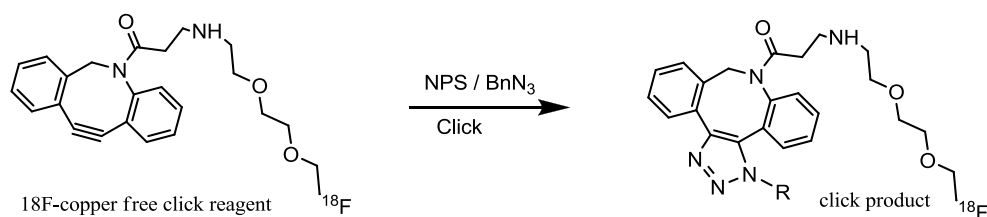


Figure 8. Radio-TLC chromatography of the SEC purified “click” product. Left, developed once; right, developed twice.

5.3.2.2.3. Radiolabeling of SCK-NP with F-18 labeled DBCO derivative using copper-free click chemistry

Copper-free click labeling of SCK-NPs with F-18 labeled DBCO derivative (Scheme 12) have been investigated. The results shown in Table 9 indicated that copper-free click chemistry significantly improved labeling efficiency. Solvent effects are also observed (Table 10). RadioTLC analysis of reaction mixture suggested that there is no wrapping of radioactivity in SCK-NPs (Figure 9), which was observed in the Cu(I) catalyzed click labeling of SCKs. Radiolabeled SCK was purified by Size exclusion column, and was identified by FPLC (Figure10).



Scheme 12. Copper-free click labeling of SCK-NPs using F-18 labeled DBCO derivative.

Table 9 Summar of copper-free click labeling with F-18

50 μ L the F-18labeled copper free reagent	100 μ L Azide sloution	Labeling yield			comments
		10 mins	20 mins	30 mins	
In MeCN	BnN3	~90	~95	-	
	NL-iv-32B	~35	~45	~60	
	SS-i-10A	~30	~35	~55	
	Non-clickable NPs	~3	~5	~8	Wrapped into NPS
In DMSO	BnN3	~80	~90	-	
	NL-iv-32B	~50	~60	~75	
	SS-i-10A	~35	~45	~60	
	Non-clickable NPs	~2	~3	~4	Wrapped into NPS

Table 10. Solvent effect for the click reaction.

SCK 22 μ M	DBCO-F18 ~ 0.5 μ M*	DMSO:H ₂ O (v : v)	SCK:DBC O-F18 (v:v)	SCK Equivalen t	Incorporatio n yield
NL-iv-32B		3 : 1	1 : 1	40	3.0 %
		1 : 1	1 : 1	40	16.5% (n=2)
		1 : 1	2 : 1	80	33%
		1 : 3	1 : 1	40	32%
		1 : 4	3 : 1	120	50%
		1 : 4	4 : 1	160	68%

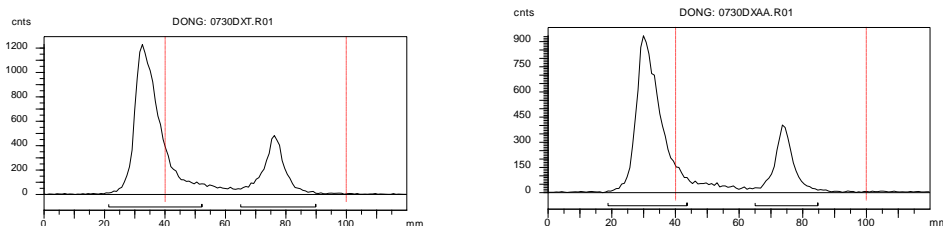


Figure 9. RadioTLC of reaction mixture of copper-free click labeling of SCKs: Left, developed once; Right, developed twice.

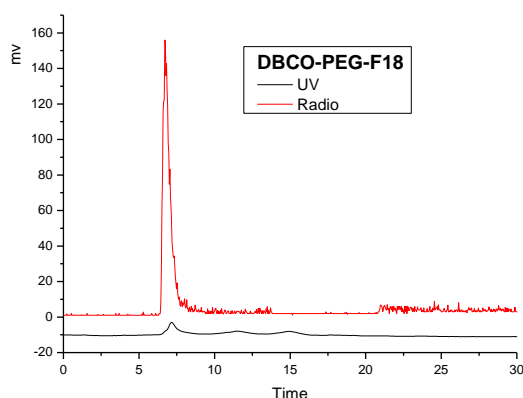


Figure 10. FPLC chromatograph of F-18 labeling SCK using copper-free chemistry.

5.3.2.2.3. Optimization of copper-free click chemistry using F-18 label DBCO

The DBCO derivative as shown in Figure 11 has been used to optimize the labeling condition of SCK-NPs due to the daily availability of F-18 and high yield of radiosynthesis of DBCO derivative. The solvent effect has been investigated using DMSO/water. As shown in Figure 12, 10 % DMSO in water afforded the best yield within 15 min at 60 °C. A saturation study has been used to determine how many copies of DBCO derivative can react inside the core of SCKs. It was estimated that about 150 copies of DBCO derivative can react inside the core within 15 min. As shown in Figure 14, up to 20 % of alkyne in the shell has minimum influence on the radiolabeling. Therefore, the optimized condition has been used for Cu-64 labeling of SCK-NPs using copper-free chemistry.

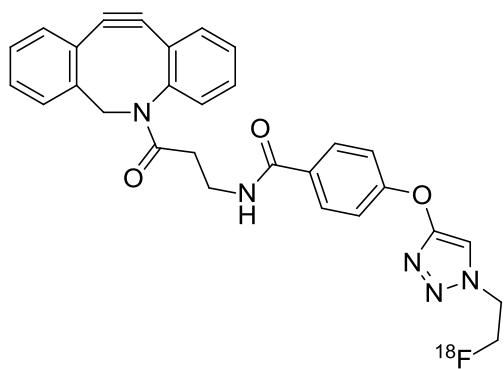


Figure 11. F-18 labeled DBCO derivative from NHS ester

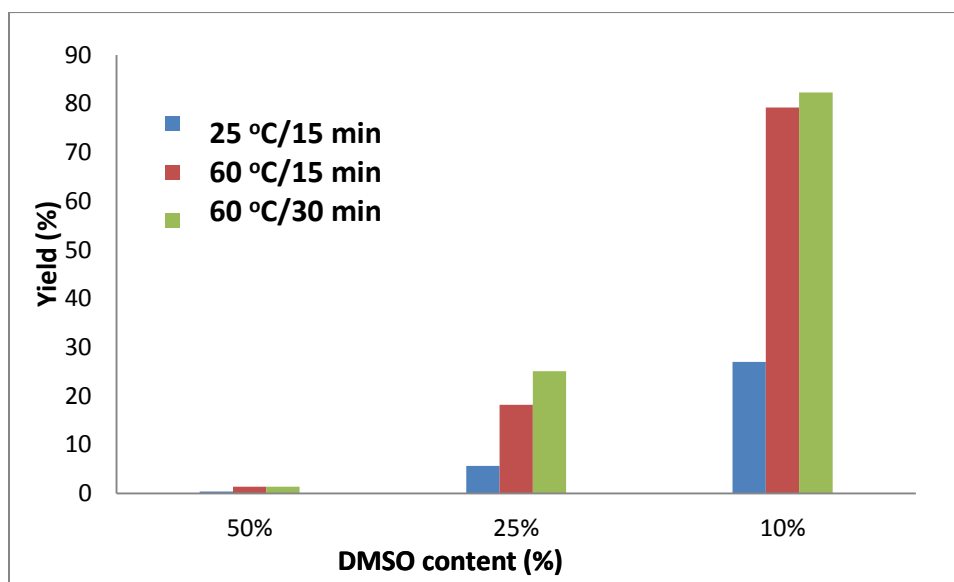
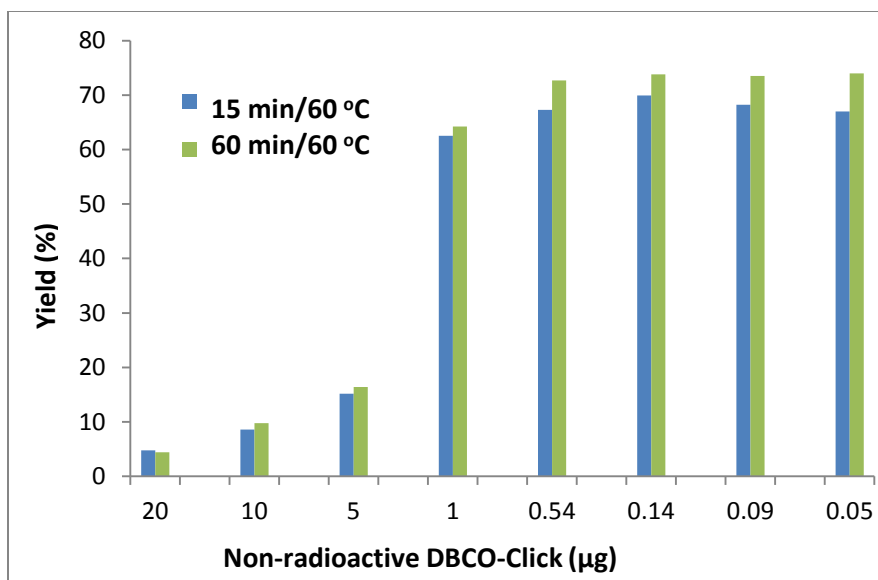
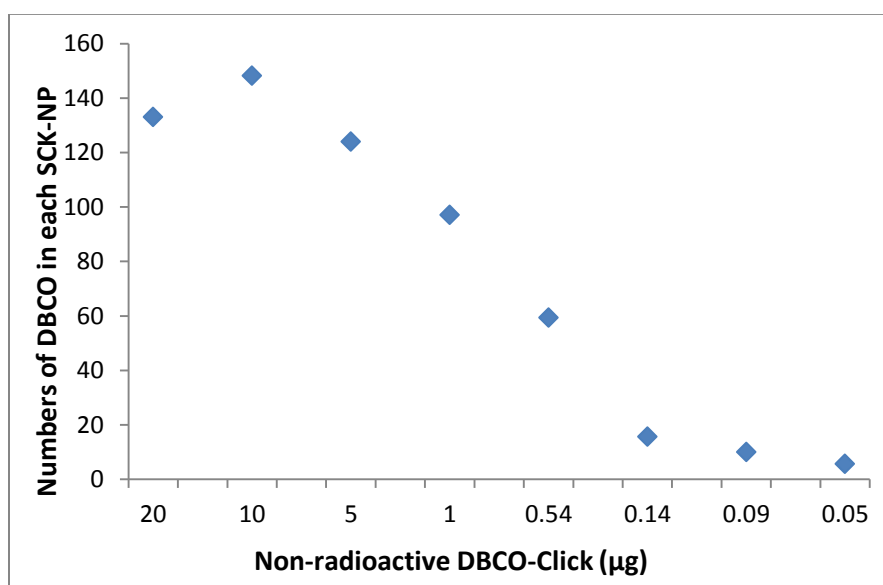


Figure 12. Solvent effect on radiolabeling of SCK-NPs using copper-free click chemistry.



(a)



(b)

Figure 13. Conjugation of SCK-NP with non-radioactive DBCO-click added: (a) Yields of incorporation with non-radioactive DBCO-click added; (b) numbers of DBCO-click in each SCK-NP

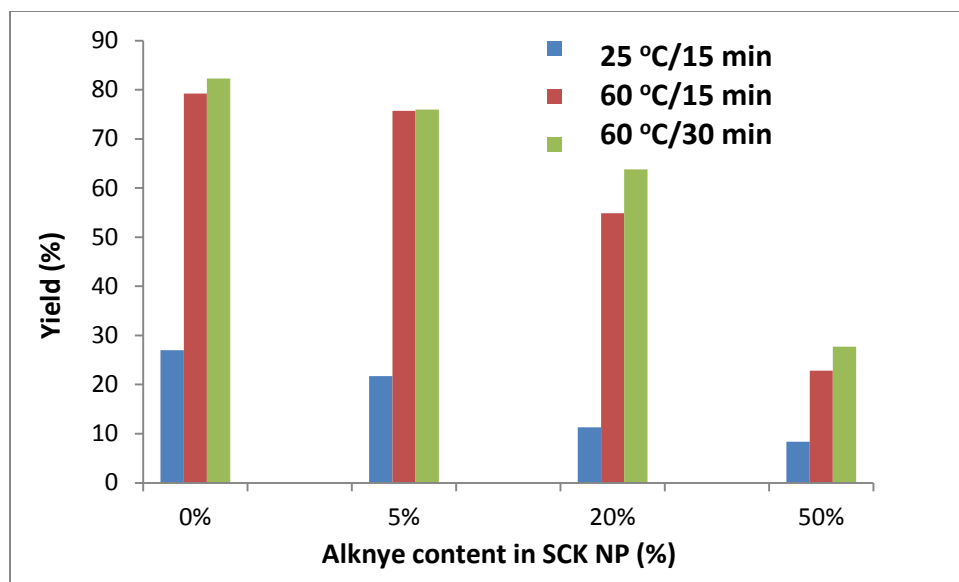
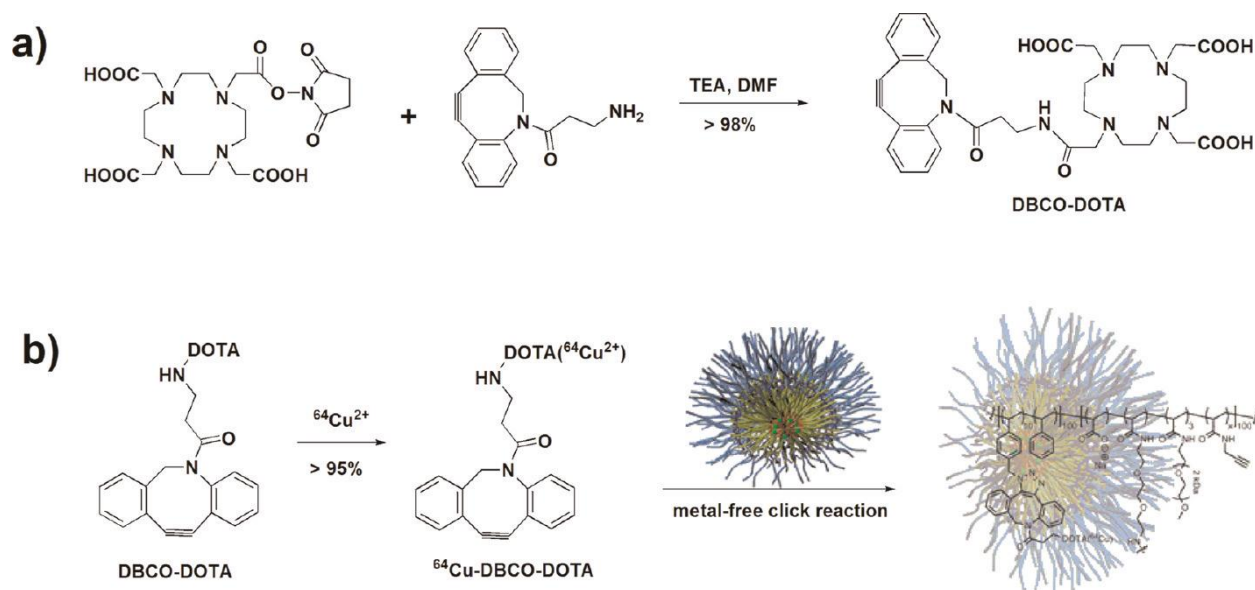


Figure 14. Influence of % of alkyne content in the shell of SCK-NPs

5.3.2.2.4. Copper-free click labeling of SCK-NPs with Cu-64

As shown in Scheme 13, a novel strategy based on metal-free “click” chemistry was developed for the copper-64 radiolabeling of the core in shell-cross-linked nanoparticles (SCK-NPs). Compared with Cu(I)-catalyzed click chemistry, this metal-free strategy provides the following advantages for Cu-64 labeling of the core of SCK-NPs: (1) limitation of copper exchange between nonradioactive Cu in the catalyst and DOTA-chelated Cu-64; (2) elimination of the internal click reactions between the azide and acetylene groups in the same NPs; and (3) increased efficiency of the click reaction because water-soluble Cu(I) does not need to reach the hydrophobic core of the NPs. When 50 mCi Cu-64 was used for the radiolabeling, the specific activity of the radiolabeled product was 975 Ci/μmol at the end of synthesis, which represents the attachment of ca. 500 Cu-64 atoms per SCK-NP, giving in essence a 500-fold amplification of specific activity of the NP over that of the Cu-64 chelate. To the best of our knowledge, this is the highest specific activity obtained for Cu-64-labeled nanoparticles.



Scheme 13. (a) Synthesis of a DOTA-attached DBCO derivative. b) Radiosynthesis of Cu-64-labeled SCK-NPs. Preparation of the DBCO-DOTA(Cu-64)

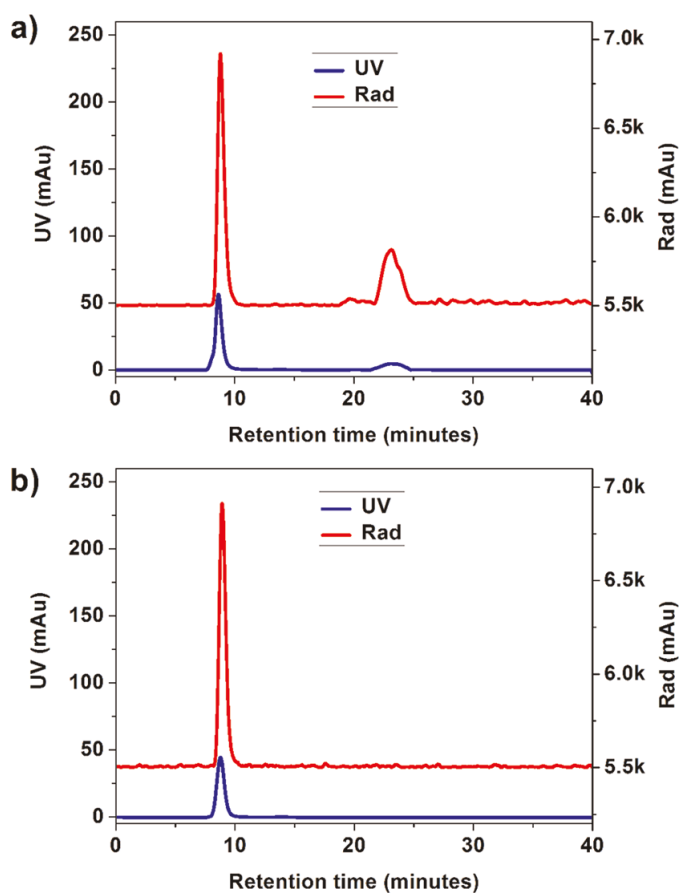


Figure15. (A) FPLC chromatography of 250 μCi of the crude metal-free click mixture before passing over a Zeba desalting column. The lack of precise peak overlap is due to interdetector flow delay. (B) FPLC chromatography of 130 μCi of the Cu-64-labeled SCK-NPs after passage over a Zeba desalting column.

5.4. Evaluate Strategies for Minimizing Autoradiolytic Damage to SCK-NPs

5.4.1. Introduction

Multiply-labeled radiopharmaceuticals are particularly prone to autoradiolytic damage, not only because of the high density of radionuclide, but also because if decay causes damage, the damaged material is still radioactive. Although the radiolytic stability of radiopharmaceuticals is often not routinely investigated carefully. In our proposed studies, we will examine two aspects of radiolysis, release of low molecular weight radioactive components and alteration of NP size as a function of decay. The former process would correspond to local damage that results in cleavage of only a small portion of the NP; the latter would represent more profound damage to the NP. *We hypothesize that because of their size and unique core-shell structure, and because the shell is extensively cross-linked, the SCK-NPs will prove to be quite resistant to autoradiolytic damage.* In addition, inclusion of radical scavengers should afford additional protection. Also, the two radionuclides we will be studying (Cu-64 and F-18) have different decay schemes and could thus prove to be quite different in terms of engendering autoradiolysis. Our systematic approach should enable us to assess the stability of the SCK-NPs, multiply labeled at high specific activity, towards autoradiolytic damage and establish how best this degradation might be minimized.

5.4.2. Results

The proposed studies have not been done due to the availability of SCK-NPs labeled with high dose of radioactivity of F-18 or Cu-64 in the proposed period.

5.5. Prepare and Evaluate High Specific Activity Cu-64 and F-18 Labeled SCK-NPs Optimally Targeted to Carbonic Anhydrase 12.

5.5.1. Introduction

While this project is focused on fundamental aspects of developing novel nuclear imaging agents for detecting low abundance biomarkers, as an advanced aim, we will evaluate the behavior of our specific activity-optimized and autoradiolytic-resistant SCK-NPs in a realistic biomarker target system. Thus, we will prepare SCK-NPs targeted to carbonic anhydrase 12 (CA12) and evaluate them in biodistribution studies. CA12 is a gene product that is highly regulated by

estrogens in breast cancer and is considered an important marker for hormone-dependent cancers that are good candidates for endocrine therapies. Being able to image CA12 levels directly in tumors by PET could give important predictive information useful in selecting the best therapy for individual breast cancer patients.

Preparation of Targeting Elements: Synthesis of Azide- and Alkyne-Substituted Ligands for Carbonic Anhydrase12, a Low-Abundance Biomarker Target for High Specific Activity SCK-NPs

To target SCK-NPs to CA12, we will prepare analogs of two known ligands for CA12 (39) that are functionalized with azide or alkyne groups (**Scheme 7**). The first of these is based on acetazolamide, a CA inhibitor in clinical use; the second is based on *p*-aminomethylbenzene sulfonamide, reported to be a specific CA12 inhibitor.

Preparation of SCK-NPs Substituted by Click Chemistry at the Shell with CA12 Ligands and Evaluation of their Binding to CA12.

SCK-NPs will be substituted with the CA12-targeting moieties by Click chemistry, using the same strategies used in the radiolabeling.

Preparation and Evaluation of CA12-Targeted High Specific Activity Cu-64 or F-18 Radiolabeled SCK-NPs for Interaction with CA12 in Breast Cancer Cells

We will next examine the interaction of the SCKs targeted to CA12 with human breast cancer MCF-7 cells. This will be done in cultures of MCF-7 cells grown either in the absence of estrogen (low CA12) or after 24 hours of treatment with 10 nM estradiol (high CA12).

Evaluation of CA12-Targeted Cu-64 or F-18 Radiolabeled SCK-NPs for In Vivo Imaging of CA12 in an Animal Model of Breast Cancer

We will examine the uptake of CA12-targeted high specific activity radiolabeled SCKs in MCF-7 xenografts grown in ovariectomized athymic mice. This is a well established tumor xenograft model of human breast cancer, and biodistribution can be studied using both μ PET imaging and standard tissue biodistribution methods. There is also strong induction of CA12 (mRNA and protein) in this model.

These studies need to be done carefully. The xenografts grow only with estrogen supplementation, which involves subcutaneous implantation of a high

dose pellet of estradiol (a cholesterol pellet containing 2 mg of estradiol, typically replaced by a pellet with 0.5 mg estradiol after tumors first appear), which generates premenopausal estrogen levels (2-3 nM). To image *changes* in the level of CA12, the estrogen pellet in some animals would be removed for 4 days (sufficient to lower estradiol levels and return CA12 levels to unstimulated levels). The uptake of the agents in tumors in the withdrawn animals (low target levels) would be determined. This would be compared with uptake in animals that received three daily doses of estradiol (5 µg SC in old), a dose that is sufficient to restimulate CA12 to maximum levels.

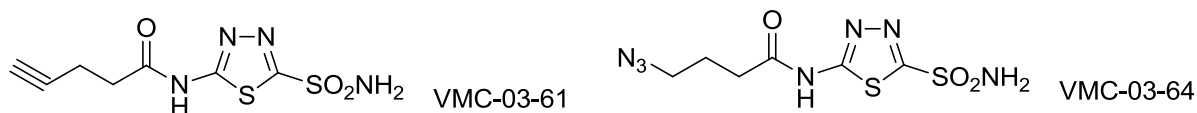
We will use µPET imaging to look at the uptake of Cu-64 and F-18 labeled SCK-NPs in tumors in withdrawn and restimulated animals. Because µPET imaging is not terminal, uptake measurements could be done in the same tumors before estrogen withdrawal, after withdrawal, and then after restimulation. By comparing uptake levels in the same tumors in the same animals, we would be able to better quantify how uptake correlates with changes in CA12 levels. Again, while we will have a good idea of the number of CA12 ligands per NP that are optimum for interaction with CA12 in solution and for cells in culture, we will also examine some variations on this optimum in performing these *in vivo* studies.

5.5.2. Results

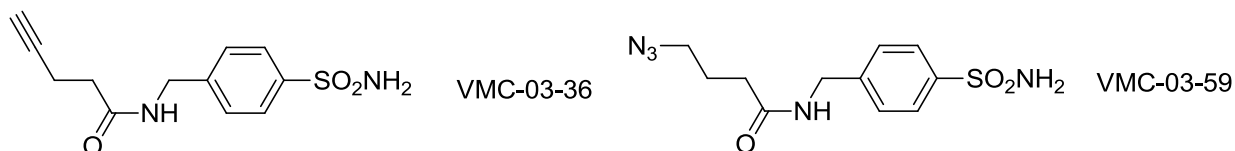
5.5.2.1. Synthesis of Azide- and Alkyne-Substituted Ligands for Carbonic Anhydrase 12

The following selective and non-selective carbonic anhydrase 12 inhibitors have been synthesized as proposed.

Non-selective carbonic anhydrase inhibitors



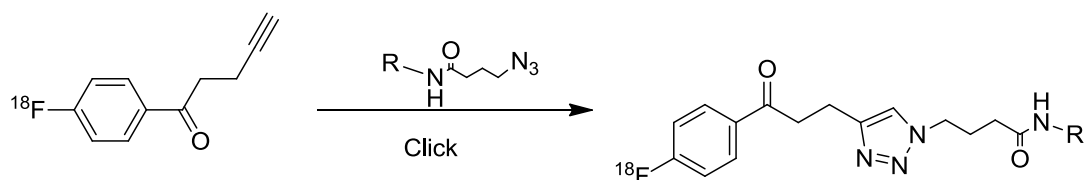
Selective carbonic anhydrase 12 inhibitors



Scheme 14. Selective and non-selective carbonic anhydrase inhibitors

5.5.2.2. Click radiolabeling of CA12 ligands with F-18 and Cu-64

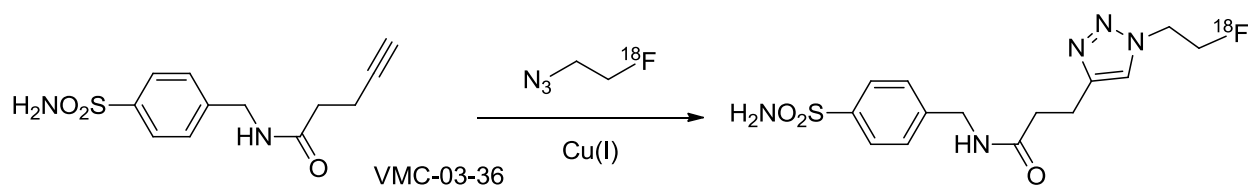
CA12 selective and non-selective ligands have been labeled with F-18 and Cu-64 using Cu(I) catalyzed click chemistry or copper-free DBCO chemistry according to Scheme 15, 16, and 17. Some of the click labeling conditions are shown in Tabel 11, which will be used for attaching CA ligands to SCK-NPs. Because of the featur of 2-[F-18]fluoroethyl azide, it was used to label VMC-03-36 in high yield, and chemical and radiochemical purities. Therefore, it was used for in vivo animal studies.



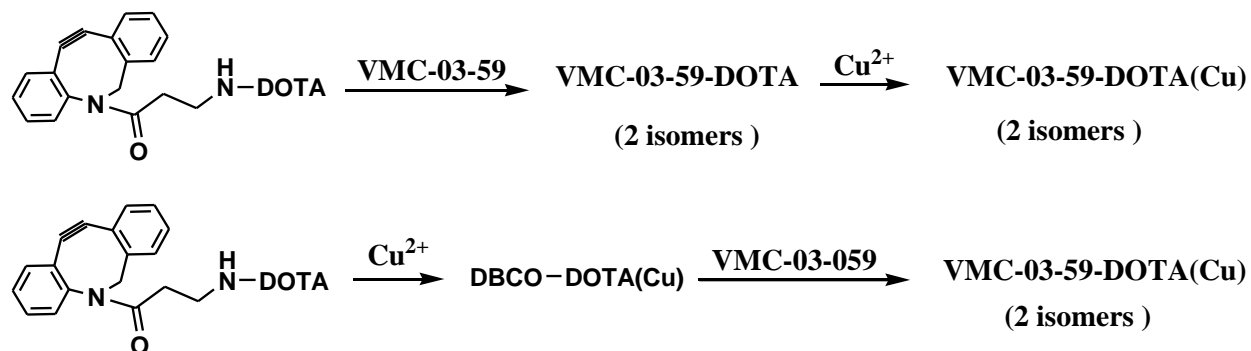
Scheme 15. Radiolabeling of CA12 ligands using Cu(I) catalyzed click chemistry

Table 11. Summary of click labeling of CA12 ligand

Sample: (0.1 mg in 50μL DMF)	catalysis	Sodium ascorbate	Labeling yield		comments
			@15 mins	@40 mins	
<p>VMC-03-64</p>	Cu(II) itself, (400 mM, 50 μL)	1.5 M, 50μL	~100%	N/A	2*10⁴ nanomole Cu (II), 7.5*10⁴ nanomole NaAscorbate
	Cu(II)-TBTA, (5mM, 10 μL)	10mM, 10μL	~100%	N/A	5*10¹ nanomole Cu(II) 1*10² nanomole NaAscorbate
	Cu(II)-BPDS, (5mM, 10 μL)	5mM, 10μL	~74%	~53%	It seems that catalysis TBTA is better than BPDS for this compound.
		5mM, 100μL	~74%	~51%	
	Cu(II)-BPDS, (5mM, 50 μL)	5mM, 100μL	~71%	~65%	
<p>VMC-03-59</p>	Cu(II) itself, (400 mM, 50 μL)	1.5 M, 50μL	~80%	~85%	2*10⁴ nanomole Cu (II), 7.5*10⁴ nanomole NaAscorbate
	Cu(II)-TBTA, (5mM, 10 μL)	10mM, 10μL	~62%	~60%	5*10¹ nanomole Cu(II) 1*10² nanomole NaAscorbate
	Cu(II)-BPDS, (5mM, 10 μL)	5mM, 10μL	0	0	It seems that catalysis TBTA is also better than BPDS here.
		5mM, 100μL	~25%	~20%	
	Cu(II)-BPDS, (5mM, 50 μL)	5mM, 100μL	~80%	~75%	



Scheme 16. Radiolabeling of selective CA12 ligand (VMC-03-36) with F-18 using click labeling of 2-[F-18]fluoroethyl azide.



Scheme 17. Radiolabeling of selective CA12 ligand (VMC-03-059) with Cu-64 using DBCO-DOTA-Cu-64.

5.5.2.3. Evaluation of F-18 labeled CA12-Targeted for In Vivo Imaging of CA12 in an Animal Model of Breast Cancer

Fluorine-18 labeled CA12 selective ligand VMC-03-059 was used for in vivo studies in order to establish and validate animal models for CA12.

Twenty days prior to imaging, 20 female Fox Chase CB-17 SCID mice received inoculation of SKOV3 tumor cells from cell culture at a concentration of $1 \times 10^6/100\mu\text{L}$ subcutaneously in the right flank area. Mice are anesthetized using a Plexiglas chamber flowing with 1 ½-2% Isoflurane and Oxygen prior to injection of Radiolabeled tracer and blocking agent (5 mg/Kg cold standard). Five seconds after the microPET® acquisition begins; the two mice are injected with $60\mu\text{Ci}/100\mu\text{L}$ of F-18 VMC-03-59 and scanned for 60 minutes. Once the scan is completed the animals are sacrificed and the following organs are harvested, weighed, and then counted on a calibrated Beckman 8000 Gamma Counter: blood, lung, kidney, muscle (abdomen), bone (tibia/fibula), uterus, ovaries, and tumor. Percent injected dose is calculated for each organ and image analysis is completed. Three additional tumors are harvested and flash frozen in liquid Nitrogen to be

analyzed for receptor concentration. In addition to the microPET®/CT studies a biodistribution was performed (n=4/group) at 15 minutes, 1 hour, and 3 hours post injection of 5 μ Ci/100 μ L. A blocking dose (5 mg/Kg cold standard) was also given to a 1 hour group of animals.

As shown in Figure 16,17 and 18, 2 h block at the high imaging dose (60 μ Ci) seems to reduce uptake all organs, though ovaries and tumors are blocked a bit more; kidney block is very good. Block is less evident at 1 h in the low dose animals (5 μ Ci); early kidney activity is very high. Blood is high in all cases, as might be expected.

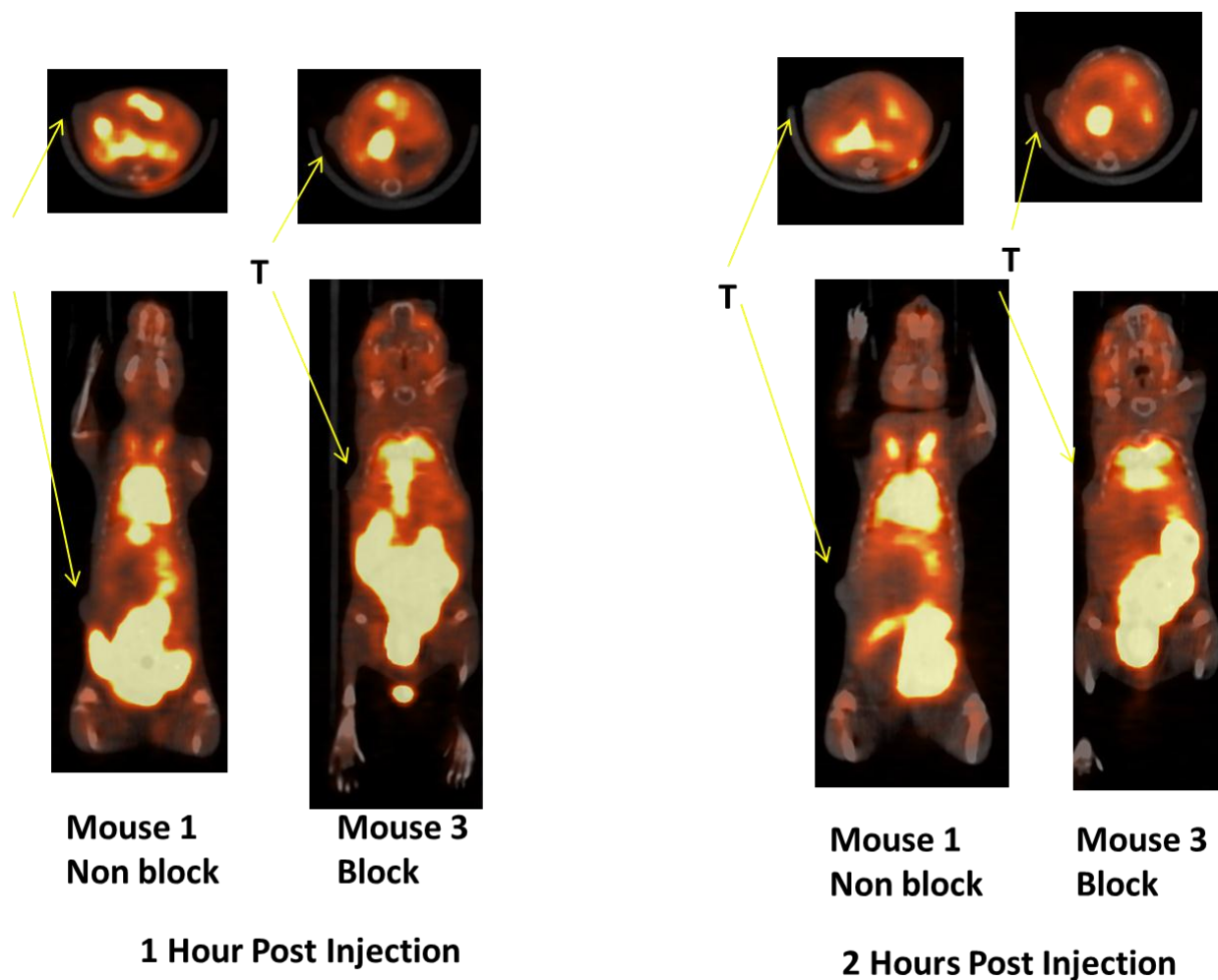


Figure 16. MicroPET image of SKOV-3 tumors in female Scid mice

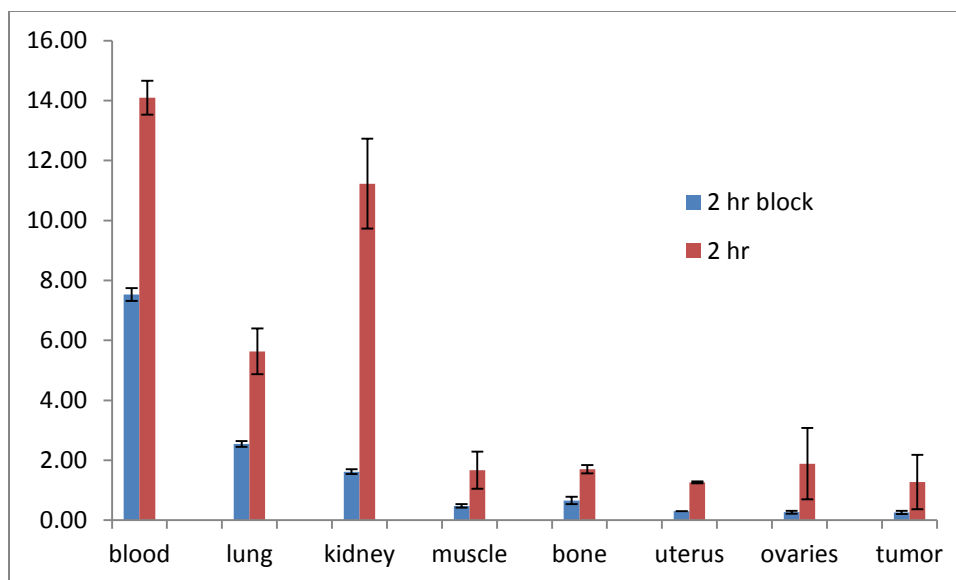


Figure 17. Post PET biod of [F-18] VMC-03-59 (CA 12) in female SCID mice with SKOV-3 tumors. (Injection dose: 60 μ Ci, Blocking dose: 5 μ g)

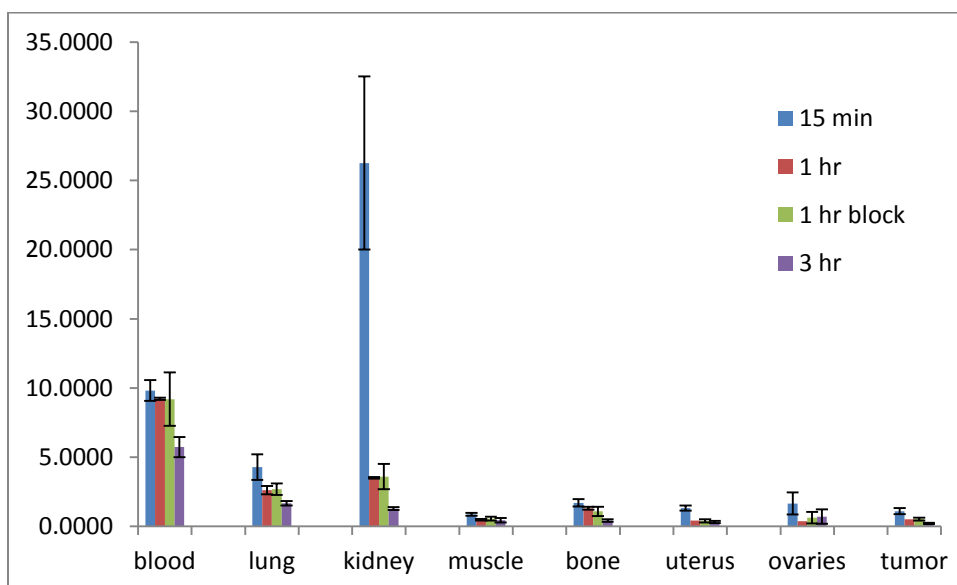


Figure 18. Biodistribution of [F18]VMC-03-59 (CA12) in female SCID mice with SKOV-3 tumors (Injected dose: 5 μ Ci, Blocking dose: 5 μ g)

SKOV3's will be looking at the various stages of hypoxia and oxygenation within the tumor along with the positive CA12 levels, it was determined that the

nesthesia at 100% oxygen could have been affecting the uptake and clearance of the tracer in all tissues as well as the tumor. This study will address those issues.

The female SCID mice were implanted with SKOV-3 cells in the right flank. The treated animals were given a pretreatment of 5mg/kg of Hydralazine IP 1 hour before F18 injection. The animals that were imaged were injected with 200 μ ci and the biodistribution animals were injected with 5 μ ci. As shown in Figure 19 and 20, 1 h at high dose (200 μ Ci), kidney is super high; no difference between oxygen and room air; hydralazine treatment increases lung, kidney, muscle, uterus, ovary, but not tumors. At low dose (5 μ Ci), all uptakes are the same.

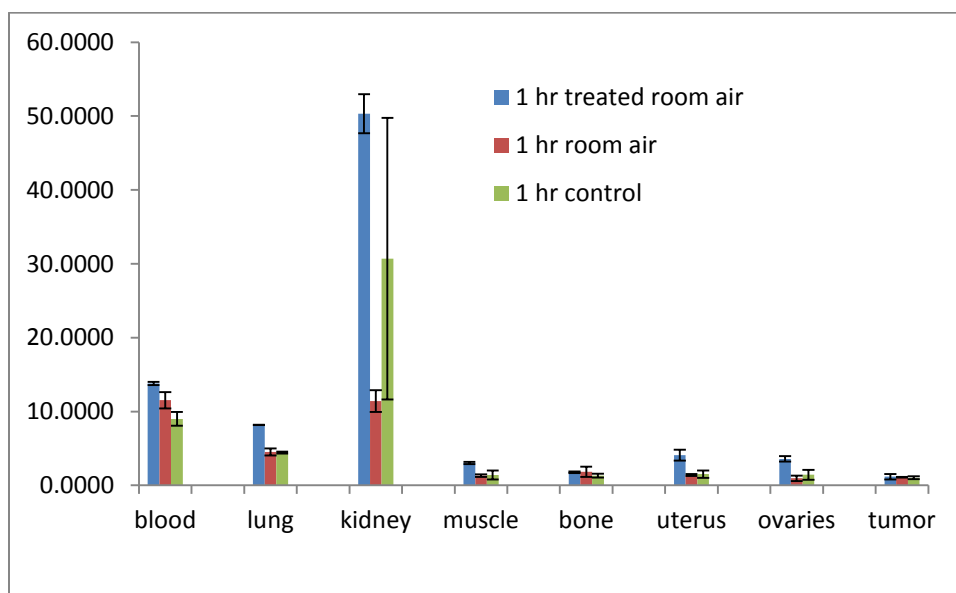


Figure 19. Post PET biodistribution of [F18] VMC-03-59 (CA-12) in female Scid mice with SKOV-3 tumors in their right flank.

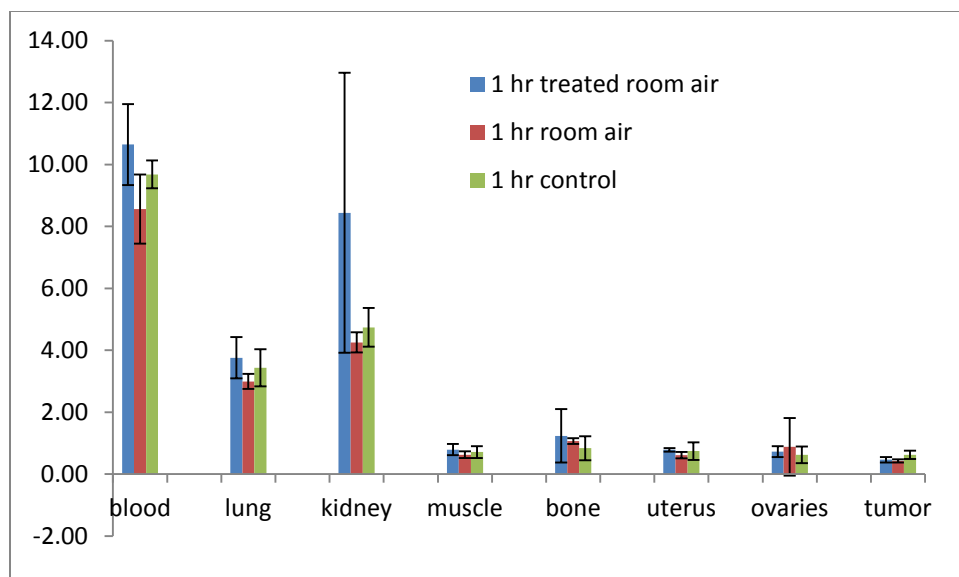


Figure 20. Biodistribution of [F-18]-VMC-03-59(CA12) in male mice with SKOV-3 tumor.

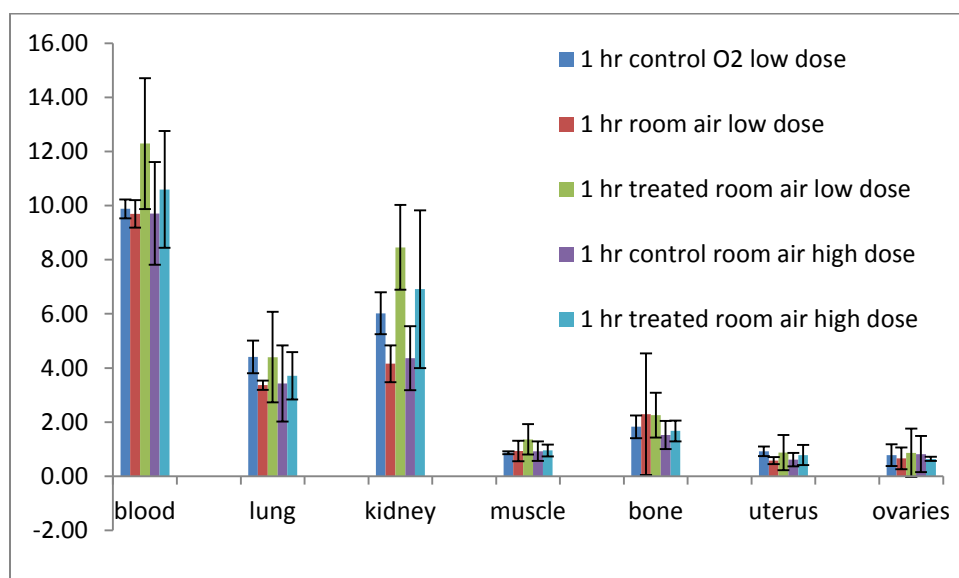


Figure 21. Biodistribution of [F-18]-VMC-03-59 (CA12) in Fox Chase Scid female mice.

The treated animals were given 5mg/kg of Hydralazine IP 1 hour before F18 injection. The high dose animals were injected with 200 μ ci and the low dose animals were injected with 6 μ ci. As shown in Figure 21 and 22, at high dose (200

μCi), no effect of hydralazine; at low dose ($6 \mu\text{Ci}$), if anything, oxygen is higher than room air; hydralazine shows modest increase in kidneys, uterus, and ovaries. Biod in non-tumor bearing animals to see if there was a blocking effect when using a higher dose (imaging dose) when compared to a low dose (biod dose). Again the animals were compared with a treatment group of hydralazine. There wasn't any significant differences between the low and high dose groups.

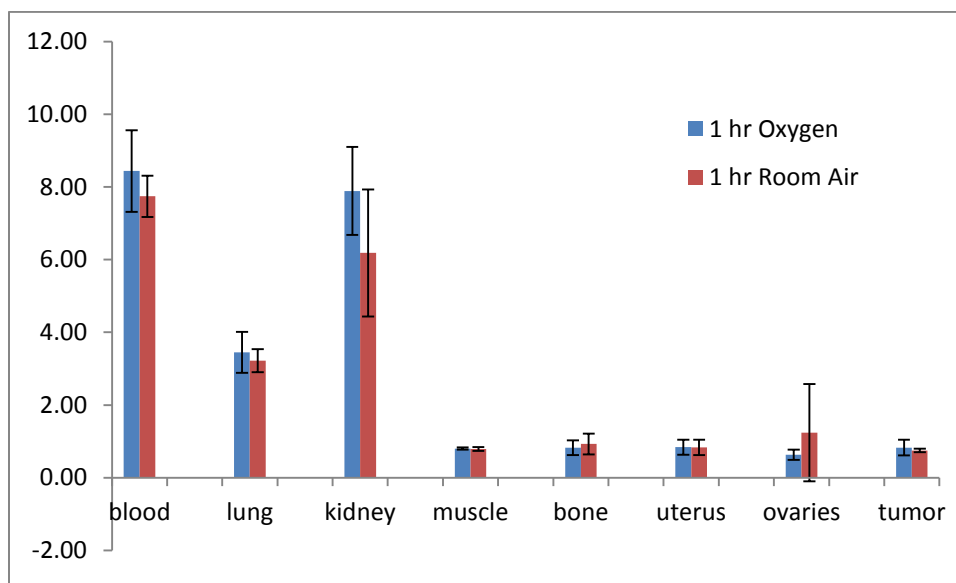


Figure 22. Biodistribution of [F18] VMC-03-59 (CA12) in female Scid mice with T47D tumors.

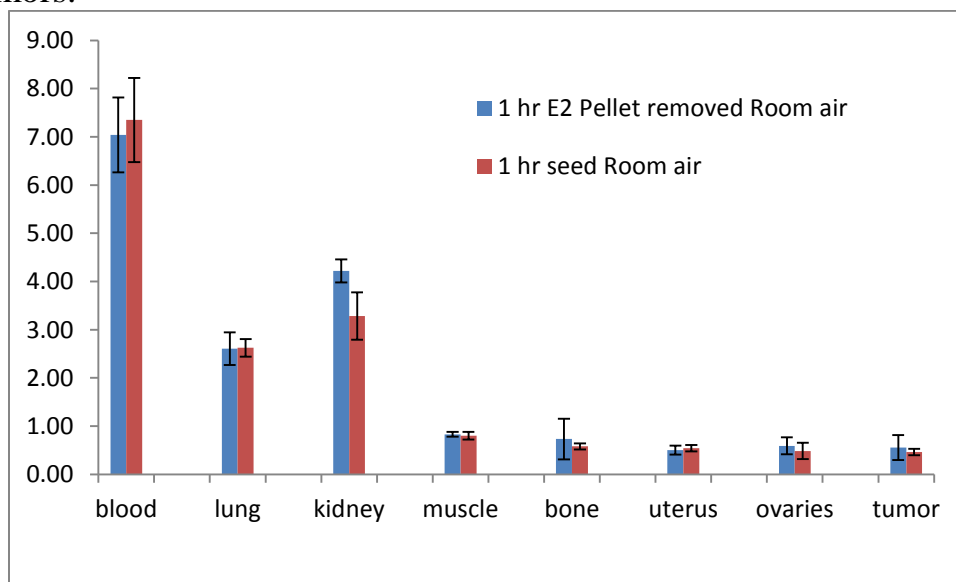


Figure 23. Biodistribution of [F18] VMC-03-59 (CA12) in female Scid mice with T47D tumors.

The female SCID mice were implanted with 0.5mg estradiol pellets. They were then implanted with T47D cells in the right flank. The pellet was removed from the E2 pellet removed group. All the other animals still had their 0.5mg pellet at sacrifice time. The SERD group was injected with 5mg of Fulvestrant SQ two days before imaging. According to Figure 22 and 23, no effect of air vs oxygen was observed. In room air, removal of estrogen pellet or SERD treatment lowers kidney, uterus, ovaries, and tumor. This is the first experiment to probe estrogen regulation of CA12.

5.6. Conclusion

We have developed a novel method to label SCP-NPS using copper-free click reaction in super high specific activity with administrable amount of final dose. The in vivo imaging of CA12 needs more effort to establish animal models.

Publication:

1. “⁶⁴Cu Core-labeled nanoparticles with high specific activity via metal-free click chemistry” ACS Nano, 2012, 6, 5209-19. doi: 10.1021/nn300974s.
2. D. Zhou, W. Chu, C. S. Dence, R. H. Mach, M. J. Welch. “Highly efficient click labeling using 2-[¹⁸F]fluoroethyl azide and synthesis of an [¹⁸F]N-hydroxysuccinimide ester as conjugation agent.” Nucl Med Biol. 2012, 39, 1175-81. doi: 10.1016/j.nucmedbio.2012.06.002.

Conference Papers:

1. D. Zhou, Y. Liu, V. Carroll, C. Dence, J. Katzenellenbogen, M. Welch. “Highly efficient radiolabeling/conjugation of PAMAM dendrimers with ¹⁸F labeled N-hydroxysuccinimide esters catalyzed by ion-ion interactions.” Presented at the SNM 59th annual meeting: Miami Beach, Florida, June 9-13, 2012, No 1554.
2. D. Zhou, W. Chu, J. McConathy, M. J. Welch, R. H. Mach. “Improved isolation of [F-18] fluoroethyl azide for click labeling reactions.” Presented at the 19th International Symposium on Radiopharmaceutical Sciences meeting: Amsterdam, the Netherlands, Aug 28-Sept 2, 2011, P-407.
3. D. Zeng, D. Zhou, N. S Lee, Y. Liu, C. S. Dence, K. L. Wooley, J. A. Katzenellenbogen, M. J. Welch. “Novel strategy for preparing Cu-64/F-18 labeled nanoparticles with ultrahigh specific activity using metal-free click chemistry.” Presented at the 19th International Symposium on Radiopharmaceutical Sciences meeting: Amsterdam, the Netherlands, Aug 28-Sept 2, 2011.
4. D. Zhou, D. Zeng, N. Lee, C. Dence, K. Wooley, J. Katzenellenbogen, M. Welch, “Fluorine-18 radiolabeling of SCK nanoparticles via copper-free click chemistry.” Presented at the SNM 58th annual meeting: San Antonio, Texas, June 4-8, 2011, No 569.
5. D. Zeng, N. Lee, Y. Liu, D. Zhou, C. Dence, K. Wooley, J. Katzenellenbogen, M. Welch, “Novel strategy for preparing Cu-64 nanoparticles with ultrahigh specific activity using metal-free click chemistry.” Presented at the SNM 58th annual meeting: San Antonio, Texas, June 4-8, 2011, No 569.

References:

1. Pressly, E.D., Rossin, R., Hagooly, A., Fukukawa, K., Messmore, B., Welch, M.J., Wooley, K.L., Lamm, M.S., Hule, R.A., Pochan, D.J. and Hawker, C.J. Structural effects on the biodistribution and positron emission tomography (PET) imaging of well-defined ^{64}Cu -labeled nanoparticles comprised of amphiphilic lock graft copolymers. *Biomacromolecules* 8:3126-3134, 2007.
2. Rossin, R., Pan, D., Kai, Q., Turner, J.L., Sun, X., Wooley, K.L. and Welch, M.J. ^{64}Cu -labeled folate conjugated shell cross-linked nanoparticles for tumor imaging and radiotherapy: Synthesis, radiolabeling and biologic evaluation. *J. Nucl. Med.* 46:1210-1218, 2005.
3. Nahrendorf, M., Zhang, H., Hembrador, S., Panizzi, P., Sosnovik, D.E., Aikawa, E., Libby, P., Swirski, F.K. and Weissleder, R. Nanoparticle PET-CT imaging of macrophages in inflammatory atherosclerosis. *Circulation* 117(3):379-387, 2008.
4. Wickline, S.A. and Lanza, G.M. Molecular imaging, targeting therapeutics and nanoscience. *J. Cell Biochem.* 87:90-97, 2002.
5. Sparreboom, Alex, Scripture, C.D., Trieu, V., Williams, P.J., De, T., Yang, A., Beals, B., Figg, W.D., Hawkins, M. and Desai, N. Comparative Preclinical and Clinical Pharmacokinetics of a Cremophor-Free, Nanoparticle Albumin-Bound Paclitaxel (ABI-007) and Paclitaxel Formulated in Cremophor (Taxol). *Clin. Cancer Res.* 11:4136-4143.
6. Harisinghani, M., Ross, R.W., Guimaraes, A.R. and Weissleder, R. Utility of a New Bolus-Injectable Nanoparticle for Clinical Cancer Staging. *Neoplasia* 9:1160-1165, 2007.
7. Joralemon, M. J., O'Reilly, R. K., Hawker, C. J. and Wooley, K. L. Shell click-crosslinked (SCC) nanoparticles: a new methodology for synthesis and orthogonal functionalization. *J. Am. Chem. Soc.* 127:16892-16899, 2005.
8. O'Reilly, R. K., Joralemon, M. J., Hawker, C. J. and Wooley, K. L. Fluorogenic 1,3-dipolar cycloaddition within the hydrophobic core of a shell cross-linked nanoparticle. *Chemistry - A European Journal* 2006, 12, 6776-6786.

9. O'Reilly, R. K., Hawker, C. J. and Wooley, K. L. Cross-linked block copolymer micelles: functional nanostructures of great potential and versatility. *Chem. Soc. Rev.* 35:1068-1083, 2006.
10. O'Reilly, R. K.; Joralemon, M. J.; Wooley, K. L.; Hawker, C. J. Functionalization of micelles and shell cross-linked nanoparticles using click chemistry. *Chem. Mater.* 17:5976-5988, 2005.